PLOS WATER

RESEARCH ARTICLE

Using detrending to assess SARS-CoV-2 wastewater loads as a leading indicator of fluctuations in COVID-19 cases at fine temporal scales: Correlations across twenty sewersheds in North Carolina

Kelly Hoffman[1☯], David Holcomb[1,2☯], Stacie Reckling[3,4], Thomas Clerkin[5], Denene Blackwood[5], Rachelle Beattie[5], Francis de los Reyes[6], Angela Harris[6], Helena Mitasova[4,7], Nadine Kotlarz[8], Jill Stewart[1], Jacob Kazenelson[9], Lawrence Cahoon[9], Arthur Frampton[9], Mariya Munir[10], Allison Lee[1], Steven Berkowitz[3], Rachel Noble[1,5], Virginia T. Guidry[3], Lawrence Engel[2‡], Marc Serre[1‡], Ariel Christensen[2,3‡*]

1 Department of Environmental Sciences and Engineering, University of North Carolina at Chapel Hill, Chapel Hill, North Carolina, United States of America, **2** Department of Epidemiology, University of North Carolina at Chapel Hill, Chapel Hill, North Carolina, United States of America, **3** North Carolina Department of Health and Human Services, Division of Public Health, Raleigh North Carolina, United States of America, **4** North Carolina State University, Center for Geospatial Analytics, Raleigh, North Carolina, United States of America, **5** Department of Earth, Institute of Marine Sciences, University of North Carolina at Chapel Hill, Marine and Environmental Sciences, Morehead City, North Carolina, United States of America, **6** Department of Civil, Construction and Environmental Engineering, North Carolina State University, Raleigh, North Carolina, United States of America, **7** Department of Marine, Earth and Atmospheric Sciences, North Carolina State University, Raleigh, North Carolina, United States of America, **8** Department of Biological Sciences, North Carolina State University, Raleigh, North Carolina, United States of America, **9** Department of Biology and Marine Biology, University of North Carolina at Wilmington, Wilmington, North Carolina, United States of America, **10** Department of Civil and Environmental Engineering, University of North Carolina at Charlotte, Charlotte, North Carolina, United States of America

☯ KH and DH are co-first authors
‡ LE, MS, and AC are co-senior authors
* ariel.christensen@dhhs.nc.gov

Citation: Hoffman K, Holcomb D, Reckling S, Clerkin T, Blackwood D, Beattie R, et al. (2023) Using detrending to assess SARS-CoV-2 wastewater loads as a leading indicator of fluctuations in COVID-19 cases at fine temporal scales: Correlations across twenty sewersheds in North Carolina. PLOS Water 2(10): e0000140. https://doi.org/10.1371/journal.pwat.0000140

Editor: Vikram Kapoor, University of Texas at San Antonio, UNITED STATES

Received: May 30, 2023

Accepted: August 14, 2023

Published: October 18, 2023

Peer Review History: PLOS recognizes the benefits of transparency in the peer review process; therefore, we enable the publication of all of the content of peer review and author responses alongside final, published articles. The editorial history of this article is available here: https://doi.org/10.1371/journal.pwat.0000140

Data Availability Statement: All wastewater data and geocoded COVID-19 cases are available by

Abstract

Wastewater surveillance emerged during the COVID-19 pandemic as a novel strategy for tracking the burden of illness in communities. Previous work has shown that trends in wastewater SARS-CoV-2 viral loads correlate well with reported COVID-19 case trends over longer time periods (i.e., months). We used detrending time series to reveal shorter sub-trend patterns (i.e., weeks) to identify leads or lags in the temporal alignment of the wastewater/case relationship. Daily incident COVID-19 cases and twice-weekly wastewater SARS-CoV-2 viral loads measured at 20 North Carolina sewersheds in 2021 were detrended using smoothing ranges of ∞, 16, 8, 4 and 2 weeks, to produce detrended cases and wastewater viral loads at progressively finer time scales. For each sewershed and smoothing range, we calculated the Spearman correlation between the cases and the wastewater viral loads with offsets of -7 to +7 days. We identified a conclusive lead/lag relationship at 15 of 20 sewersheds, with detrended wastewater loads temporally leading detrended COVID-19 cases at

date and wastewater treatment plant here - https://covid19.ncdhhs.gov/dashboard/data-behind-dashboards. Please scroll to the "wastewater monitoring" tab on the page. Then toggle to download the "viral gene copies per person" in one csv/excel file and the "new cases per 10,000 persons" in a csv/excel file.

Funding: We gratefully acknowledge the funding support provided by the Centers for Disease Control and Prevention (CDC) National Wastewater Surveillance System (NWSS) through the Epidemiology and Laboratory Capacity (ELC) Cooperative Agreement (VG, AC, SR, SB). Additionally, we acknowledge the support and foresight of Dr. Jeff Warren and the North Carolina Policy Collaboratory for the project entitled "Tracking SARS-CoV-2 in the Wastewater Across a Range of North Carolina Municipalities" which allowed NC to emerge as a leader in wastewater surveillance (RN, MS, MM, LE, AH, JS, HM, LC, AF, FR). Support was also received from the National Institute for Occupational Health and Safety (T42OH008673 to MS, LE) and the NSF RAPID program for project number 2029866 (to MS, LE) entitled "RAPID: Identifying Geographic and Demographic Drivers of Rural Disease Transmission for Improved Modeling and Decision Making". The funders had no role in study design, data collection and analysis, decision to publish, or preparation of the manuscript.

Competing interests: The authors have declared that no competing interests exist.

11 of these sites. For the 11 leading sites, the correlation between wastewater loads and cases was greatest for wastewater loads sampled at a median lead time of 6 days before the cases were reported. Distinct lead/lag relationships were the most pronounced after detrending with smoothing ranges of 4–8 weeks, suggesting that SARS-CoV-2 wastewater viral loads can track fluctuations in COVID-19 case incidence rates at fine time scales and may serve as a leading indicator in many settings. These results could help public health officials identify, and deploy timely responses in, areas where cases are increasing faster than the overall pandemic trend.

Introduction

The first lab-confirmed COVID-19 case was reported in North Carolina (NC) on March 3, 2020, and over the next two and a half years, the number of reported positive cases statewide increased to more than three million [1,2]. However, the true burden of disease far exceeded this number due to underreporting, access to testing, unreported at-home tests, asymptomatic illness and other factors [3–5]. Testing was not uniformly distributed among populations for a number of structural and cultural reasons, including unequal availability and pervasive mistrust of public health recommendations by historically marginalized persons [6–8]. As a result, there is need for non-clinical means of tracking COVID-19 trends to augment case-based reporting.

One promising approach is wastewater-based epidemiology (WBE), which measures substances shed in human feces and derived from a condition of interest, such as pathogen nucleic acids or pharmaceutical metabolites, by sampling sewage containing human fecal waste and byproducts of water usage [9]. WBE has been increasingly utilized to track COVID-19 infection trends at the community level by quantifying SARS-CoV-2 RNA in sewage. Twice-weekly testing of SARS-CoV-2 loads in wastewater can provide information on changes in COVID-19 burden in the sewershed population and can be used as a method to detect periods of increasing COVID-19 cases from far fewer samples than required for clinical case reporting since wastewater samples represent pooled samples of multiple individuals [10]. Unlike case-based surveillance, wastewater surveillance does not rely on individual healthcare-seeking behavior or access to testing, which are strongly impacted by well-documented societal inequities [11]. Additionally, SARS-CoV-2 is shed in the feces of both symptomatic and asymptomatic individuals, allowing the capture of data on a range of infected individuals [12–14] at varying stages of infection. Numerous studies have shown that when clinical testing coverage is high, wastewater SARS-CoV-2 loads and documented COVID-19 cases follow similar trends and are highly correlated [15–18]. Therefore, given the cost and human resource savings, WBE may provide an effective complement to case-based surveillance that addresses some of the limitations of traditional clinical surveillance approaches.

However, the values typically measured in wastewater, such as viral genome copies per liter, are not directly interpretable in terms of familiar population health metrics, like the prevalence or incidence rate of infection in a defined population. To effectively inform public health response and mitigation strategies using WBE, it is necessary to relate wastewater-based measurements to interpretable population-level metrics. One critical aspect is the temporal relationship between SARS-CoV-2 wastewater loads measured at a wastewater treatment plant (WWTP) and reported COVID-19 cases in the corresponding sewershed served by the plant [5,19]. Past work has demonstrated that increases in SARS-CoV-2 wastewater loads may occur prior to a rise in lab-confirmed sewershed COVID-19 cases in a sewershed, allowing for WBE

to be used as an early warning system [4,20–22]. Such leading signals in wastewater were reported during the earlier phases of the pandemic in some North Carolina sewersheds [10,23] as well as during more recent pandemic phases [24].

As the pandemic becomes endemic, trends lasting several months have been widely reported to anticipate trends in COVID-19 infections, as later indicated by population surveillance metrics [21,22,25,26]. However, the time alignment between trends in wastewater load and trends in cases can be difficult to determine since its small temporal lead or lag may be eclipsed by the longer time scale of trends. In this situation, kernel detrending can be used to remove these longer pandemic trends and reveal shorter-term fluctuations that may help identify leads or lags in the temporal alignment of the detrended wastewater and detrended case relationship [27–31]. While the correlation between wastewater-based measurements of pathogens of concern and clinical cases over longer time periods (i.e., months) is useful for informing longer-term public health response, much less is known about short-term sub-trends (i.e., weekly or even daily), which may be more relevant for ongoing, day-to-day public health decision making. Therefore, there is a need for research to better understand and anticipate changes in COVID-19 incidence on shorter time scales to inform timely, targeted, and cost-effective public health action, particularly at the local level. *Detrending* the wastewater and case data is done by modeling these longer-term trends and removing them to obtain detrended wastewater loads and detrended cases, also referred to as wastewater load residuals and case residuals, respectively. If wastewater load residuals can predict a fine-scale fluctuation in case residuals, then public health measures can be taken *locally* and for *short* durations in sewersheds where cases are anticipated to rise at levels greater than that of the baseline trend. This methodology may also be applicable for other pathogens beyond SARS-CoV-2 as wastewater surveillance expands to new targets in the future.

Our work aims to contribute to previous studies by refining the time scale at which correlations between wastewater and cases are assessed. Accordingly, we investigate the temporal relationship (i.e., lead or lag) that maximizes correlation between detrended wastewater SARS-CoV-2 viral loads and detrended COVID-19 clinical cases at the finest time-scale possible for 20 sewersheds across North Carolina in 2021. Furthermore, to operationalize this approach, we propose and validate a set of reproducible criteria that can be easily deployed by public health agencies to support the application of WBE approaches beyond North Carolina.

Materials and methods

Ongoing wastewater-based epidemiology in North Carolina

In collaboration with University of North Carolina (UNC) system researchers, the North Carolina Department of Health and Human Services (NCDHHS) was one of eight state health departments initially funded by the Centers for Disease Control and Prevention (CDC) to participate in the National Wastewater Surveillance System (NWSS). The NCDHHS NC Wastewater Monitoring Network is a multi-disciplinary collaboration between epidemiologists, laboratory scientists, water reclamation managers, environmental engineers, and public health officials with promising applications for genomic, large-scale pathogen monitoring, as well as COVID-19. The development of this state surveillance network benefited from a collaboration funded by the North Carolina State Legislature among North Carolina universities at the start of the pandemic in 2020. This group of experts created the NC Wastewater Pathogen Research Network to develop sampling techniques, laboratory capabilities, and analysis of SARS-CoV-2 in wastewater [32]. The NC Wastewater Pathogen Research Network, in collaboration with NCDHHS, established a strong foundation for WBE, and founding contributors continue to

be essential partners in the NC Wastewater Monitoring Network using a framework of innovative research to inform public health surveillance and action in North Carolina.

As part of the NC Wastewater Monitoring Network data collection in 2021, wastewater samples were collected twice per week by WWTP staff and shipped to the UNC-Chapel Hill Institute of Marine Sciences (IMS, Morehead City, NC) for laboratory analysis. Samples were analyzed for SARS-CoV-2 by reverse-transcription droplet digital polymerase chain reaction (RT-ddPCR) following a standardized protocol [33], for which additional details are provided in the Supporting Information [34]. Sewer network spatial data (e.g., gravity mains, force mains, manholes, pump stations) obtained from North Carolina wastewater utilities and local geographic information systems departments were used to delineate a sewershed polygon using ArcGIS Pro 2.8 (ESRI, Redlands, CA). COVID-19 clinical cases reported to NCDHHS were geocoded in ArcMap 10.7.1 (ESRI) and matched to the sewershed within which they resided using a custom composite geocoder built from state and county address data. Lastly, wastewater sample results and recorded clinical cases in the sewershed were submitted to NCDHHS and uploaded weekly the CDC NWSS analytics platform for epidemiologic trend analysis. COVID-19 cases were given a date based on the following hierarchy: date of symptom onset, date of specimen collection, and date of result. Daily incidence rates per 100,000 estimated sewershed population were calculated. Wastewater sample results were normalized to flow within each municipal utility to represent a 24-hour viral load. These analyzed data are posted publicly on the CDC COVID-19 Data Tracker and the NCDHHS COVID Dashboard (https://covid19.ncdhhs.gov/dashboard/wastewater-monitoring). No permits were required for this work. Wastewater treatment plants participate voluntarily in the NC Wastewater Monitoring Network.

Relating wastewater loads and COVID-19 incidence

During a ten-month study period from January 2021 through October 2021, we compared SARS-CoV-2 viral loads in influent wastewater collected at the 20 WWTPs in the NC Wastewater Monitoring Network with COVID-19 incidence in the corresponding sewersheds. Nine sites were sampled for the entire duration of the study period, two sites were sampled beginning in January and ending before October 2021, and nine sites were added in the summer and sampled from June 2021 through October 2021 (Table 1). We retrieved calculated wastewater viral loads and clinical COVID-19 incidence rates in the sewershed for each of the 20 sites from the CDC NWSS analytics platform. Twice-weekly wastewater loads were provided as the sample-specific geometric mean of measured N1 and N2 target copy numbers per liter (L) of wastewater [35], normalized by multiplying by the average daily flow and dividing by the estimated sewershed population. Half the target-specific limit of detection (LOD) was substituted for the concentration when a target was not detected in the sample (N1 LOD = 1170 copies/L, N2 LOD = 330 copies/L; see Supporting Information). The resulting population-normalized viral loads, with units of SARS-CoV-2 N gene copies (GC) per person per day (pppd), were $\log_{10}$-transformed for all analyses, which were conducted in R version 4.1.2 [36]. Code for all analyses in R Markdown format is freely available in a permanent online repository at https://osf.io/gzfb5/ [37]; as all data analyzed were publicly available, this research did not involve human subjects.

Exponential kernel smoothing is a technique used in space/time geostatistics to estimate spatial and temporal trends of environmental and health processes at a variety of spatial and temporal scales [27–31]. Here, we used exponential kernel smoothing to estimate trends in wastewater viral loads and COVID-19 incidence rates at different temporal scales. For each observed response, a smoothed estimate was obtained as the average of all observations

Table 1. Characteristics of NC wastewater monitoring network sites.

WWTP Name	Population (2019)	Area (km^2)	Capacity (ML/day)	First Sample	Last Sample	Number of Samples[a]
Newport	3,731	6.1	5	1/12/2021	8/18/2021	64
Pittsboro	3,799	10.3	3	1/5/2021	5/25/2021	39
Beaufort	3,992	7.4	7	1/5/2021	10/20/2021	83
Marion	7,793	22.9	14	6/17/2021	10/14/2021	35
Laurinburg	15,407	37.4	18	6/17/2021	10/19/2021	36
Roanoke Rapids	19,335	43.9	38	6/19/2021	10/20/2021	33
Wilson	51,285	164.4	64	6/19/2021	10/19/2021	33
New Hanover Co.	51,401	81.4	48	1/22/2021	10/20/2021	78
Wilmington	65,081	62.5	25	1/5/2021	10/20/2021	79
Charlotte 1	77,278	126	55	1/5/2021	10/19/2021	76
Chapel Hill	84,729	89.8	66	1/6/2021	10/20/2021	81
Greenville	94,194	95.2	80	1/5/2021	10/20/2021	81
South Durham	98,068	100.7	91	1/6/2021	10/20/2021	81
Charlotte 3	122,063	122.2	55	6/3/2021	10/19/2021	38
Greensboro	144,539	143.6	82	6/18/2021	10/20/2021	36
Charlotte 2	154,519	105.3	127	1/4/2021	10/19/2021	80
Fayetteville	159,000	250.8	95	6/19/2021	10/20/2021	36
Winston Salem	177,520	319.6	70	6/19/2021	10/20/2021	33
MSD of Buncombe Co.	188,927	534.4	182	6/19/2021	10/20/2021	33
Raleigh	551,534	536.7	341	1/6/2021	10/20/2021	74

[a] Sites were sampled twice weekly.

https://doi.org/10.1371/journal.pwat.0000140.t001

weighted by an exponentially decaying function of the temporal distance from the estimation time point. The rate of exponential decay was determined by a smoothing range parameter, corresponding to the temporal duration below which variations in the response are smoothed out of the mean trend to retain only those variations of greater duration than the smoothing range. For a response $y(t)$ observed at time t, the smoothed estimate was obtained as the mean trend $m_y(t;T)$ with smoothing range of duration T:

$$m_y(t;T) = \sum_{j=1}^{N} k_j y\left(t_j\right) \tag{1}$$

where $y(t_j)$, $j = 1,\ldots N$, are the observations at observation times t_j and the exponential kernel smoothing weights k_j are given by

$$k_j = \frac{exp\left(\frac{-3|t_j - t|}{T}\right)}{\sum_{j=1}^{N} exp\left(\frac{-3|t_j - t|}{T}\right)} \tag{2}$$

Scaling the exponential decay function by -3 ensured that the influence of observations with temporal distance equal to the smoothing range T was diminished by ~95%, with the estimation point itself receiving the highest weight. As T increased, observations further away in time were allowed greater influence on the mean trend, increasing the extent of smoothing until converging to a constant value at the arithmetic mean of all the data for T of infinite duration.

As the mean trend $m_y(t;T)$ only retained variations in the response of greater duration than the smoothing range T, we detrended the observed responses by subtracting the mean trend estimated at time t to obtain the residual response:

$$\tilde{y}(t;T) = y(t) - m_y(t;T) \tag{3}$$

which captured the fluctuations around the trend at temporal scales shorter than the smoothing range T (including any measurement error). In short, we decomposed the signal $y_i(t)$ into a time trend $m_{y_i}(t;T)$ that captured variation of time scales greater than T and a detrended signal $\tilde{y}_i(t;T)$ that captured fluctuations of time scale shorter than T, corresponding to the shorter-term variations around pandemic trends that are of particular relevance to timely public health action.

To examine the time scales at which wastewater signals may lead (i.e., precede) or lag (i.e., follow) clinical cases at North Carolina Wastewater Monitoring Network sites, we evaluated the cross-correlation between *detrended* wastewater viral loads, denoted $\tilde{w}(t;T)$, and *detrended* COVID-19 incidence rates $\tilde{y}(t;T)$ across various detrending kernel smoothing ranges for observations from January—October, 2021. The cross-correlation between two time series was determined as the set of correlations between pairs of observations for different temporal offsets τ, given by

$$r(\tau;T) = corr(\tilde{w}(t+\tau;T), \tilde{y}(t;T)) \tag{4}$$

for which $\tau < 0$ indicated the detrended wastewater load signal leads the detrended signal obtained from COVID-19 incidence rates; conversely, $\tau > 0$ indicated the signal from detrended wastewater loads lags that of detrended COVID-19 incidence.

We examined detrended wastewater loads and detrended COVID-19 incidence rates with detrending smoothing ranges of $T = \infty$, 16, 8, 4 and 2 weeks separately for each site. Because subtracting a constant does not affect correlation estimates, using the $T = \infty$ detrended residuals was equivalent to performing the analysis without detrending. As we anticipated nonlinear associations, we estimated Spearman's rank correlations (ρ), which are nonparametric, to assess the monotonic relationships between the two surveillance systems for temporal offsets ranging from τ = -7 to τ = +7 days. The optimal combination of detrending smoothing range and temporal offset to characterize the lead/lag relationship between wastewater and incidence over relevant time scales was identified for each site by applying a reproducible set of criteria. For each detrending smoothing range T, starting from $T = \infty$ down to T = 2, we:

1. Identified the span of consecutive lead/lag values τ for which $r(\tau;T)$ was a statistically significant positive correlation.
2. Accepted τ if (a) it was less than 7 days (identifiable), (b) it lasted at least 2 days (persistent), and (c) it contained the maximum $r(\tau;T)$ value (predictive). Otherwise, it was rejected and deemed inconclusive.

Finally, the optimal smoothing range was obtained by choosing the shortest detrending smoothing range T that successfully identified a conclusive lead or lag. Detecting fluctuations over a shorter duration is ideal because these can be addressed with more timely public health measures. We selected criteria that favor identifiability, persistence, and predictivity; however, this framework may easily be extended to additional or alternative criteria as required by the specific application.

Results

Charlotte 1 sewershed case study

In this case study, we demonstrate the use of kernel detrending in the cross-correlation analysis of SARS-CoV-2 wastewater loads and COVID-19 incidence in the Charlotte 1 sewershed. One of three WWTPs in the Charlotte metropolitan area monitored by the NC Wastewater Monitoring Network during the study period, the Charlotte 1 sewershed covers 126 km^2 in the northeast of the city and serves approximately 80,000 people. From January to October 2021, 76 wastewater samples were collected at Charlotte 1 with a SARS-CoV-2 RNA detection frequency of 98% and a mean daily load of 9.2 x 10^6 GC pppd. The maximum load was an order of magnitude higher at 4.7 x 10^7 GC pppd and the minimum load was 7.9 x 10^4 GC pppd. A total of 6,039 COVID-19 cases were reported in the Charlotte 1 sewershed over the 10-month study period, with a daily incidence rate of 30 cases/100,000 people on average and a maximum of 132 cases/100,000 people. There was only one day with zero COVID-19 cases reported (0.3%, n = 293 days).

Visual inspection of trends in the Charlotte 1 sewershed indicated the wastewater loads generally mirrored the COVID-19 incidence rates, with a peak in January, a gradual decline through July followed by a sharper increase in August and second peak around September (Fig 1a and 1b). The mean trend was estimated at each time point for smoothing ranges of $T = \infty$, 16, 8, 4 and 2 weeks. Using $T = \infty$ resulted in a flat (i.e. constant) trend line. Then, as the kernel smoothing range became finer (i.e. T = 16, 8, 4 and 2 weeks), the trend line captured more of the inflections in the wastewater and case trends.

Subtracting the various mean trends from the wastewater and case observations yielded residuals retaining the variation in the observations at time scales shorter than the corresponding smoothing range T. With an 8-week range, the detrended wastewater loads and detrended cases (Fig 1c and 1d) demonstrated lower temporal variability compared to the variability seen without detrending (Fig 1a and 1b). Scatterplots comparing the detrended wastewater loads and detrended cases on the same day (i.e., temporal offset $\tau = 0$) are presented in Fig 1e and 1f for detrending smoothing ranges $T = \infty$ weeks and T = 8 weeks, respectively. As anticipated, we observed that the pairwise correlation between detrended wastewater loads and detrended cases declined with decreasing detrending smoothing range (i.e., as $T = \infty$, 16, 8, 4 and 2 weeks) because more of the pandemic-scale trend was removed and only shorter-term fluctuations remained. However, detrended residuals were significantly positively correlated for all detrending smoothing ranges other than T = 2 (the shortest range considered, Spearman's $\rho = 0.19$, $p = 0.11$).

We then calculated, for each detrending smoothing range T, not only the correlation for detrended wastewater observations on the same day as each case date ($\tau = 0$), but also for wastewater observations up to 7 days before ($\tau = -7$) and 7 days after ($\tau = +7$) each case date (Fig 1g). Based on our proposed criteria, we determined the shortest smoothing range T to conclusively identify a time offset τ for predicting detrended cases from detrended wastewater loads in the Charlotte 1 sewershed was T = 8 weeks, which revealed positive correlations for wastewater measured 0 to 3 days before cases were reported. This set of contiguous positive correlations spanned more than 2 and fewer than 7 contiguous days and included the maximum correlation value ($\rho = 0.40$), satisfying our proposed criteria for identifiable and predictive lead/lag relationships. Longer detrending smoothing ranges ($T = \infty$ and T = 16 weeks) demonstrated significant positive correlations at all temporal offsets, suggesting that the lead/lag relationships were not identifiable because they were dominated by overall pandemic trends that obscured the short-term fluctuations relevant to timely public health action. Conversely, the shorter 4- and 2-week detrending smoothing ranges removed so much of the trend

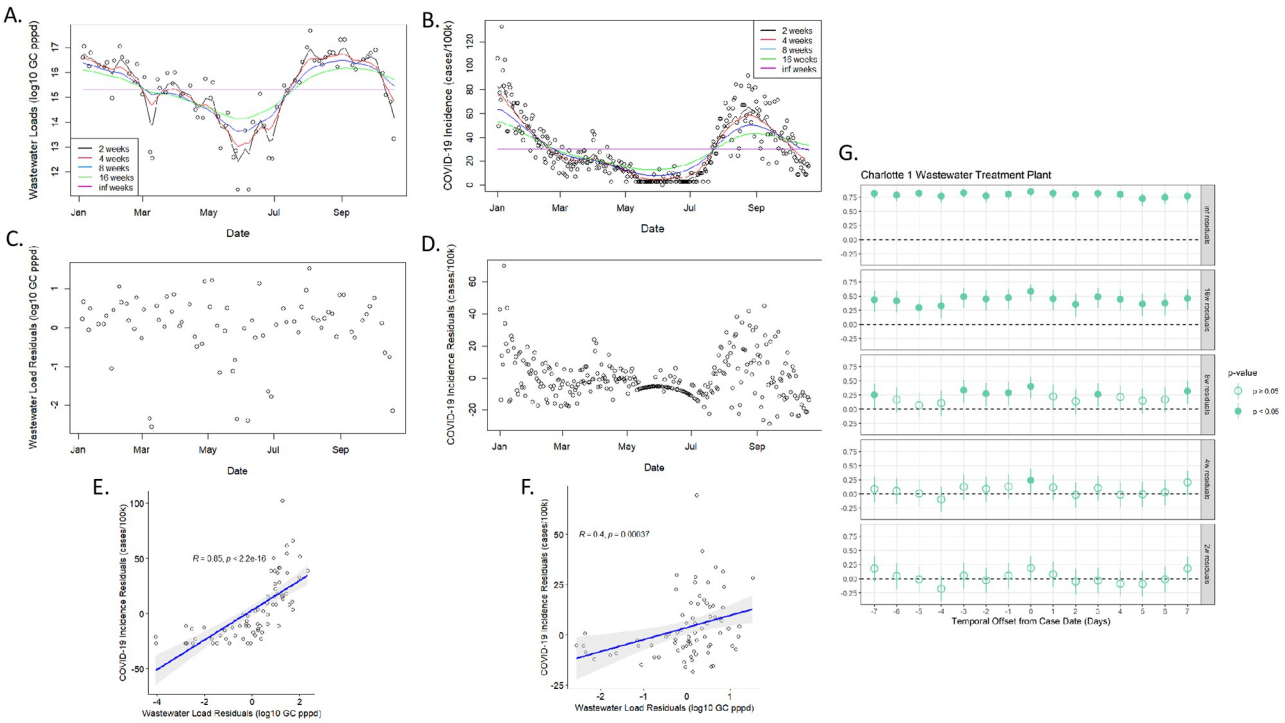

Fig 1. Kernel smoothing of the (A) SARS-CoV-2 wastewater loads (log GC pppd) and (B) COVID-19 incidence (cases/100k) observed at Charlotte 1 sewershed from January to October 2021, using various range parameters indicated by the colored lines in the legend. The smoothed estimates were subtracted from the observations to yield the (C) detrended wastewater loads and (D) detrended cases, shown here for a detrending smoothing range of 8-weeks. The pairwise correspondence of the detrended wastewater and case residuals on the same day (i.e. temporal offset of zero) were compared in scatterplots with added spearman correlation lines prior to evaluating any temporal offsets for detrending smoothing ranges of (E) $T = \infty$ weeks and (F) $T = 8$ weeks. A cross-correlation plot (G) between the detrended wastewater and case residuals was created for each detrending smoothing range and temporal offset to be used with the criteria to assess the lead/lag relationship. Note: The temporal offset values on the x-axis are in relation to the case date, such that negative values indicate the correlation was performed when the wastewater preceded the cases and positive values indicate the correlation was performed when the wastewater lagged the cases. Statistically significant correlations are indicated with a filled-in circle and the intersecting line represents the 95% confidence interval.

https://doi.org/10.1371/journal.pwat.0000140.g001

that the residuals were not predictive at any contiguous sets of temporal offsets, rendering the lead/lag relationships inconclusive. We therefore concluded that the finest detrending timescale at which wastewater loads predicted COVID-19 cases in the Charlotte 1 sewershed during our study period—based on our reproducible criteria for identifiability, persistency and predictivity—was 8-weeks, and that the correlation between detrended wastewater loads and detrended cases was greatest for wastewater loads sampled with a lead time of 0 to 3 days before the cases were reported.

Wastewater loads and COVID-19 incidence across all sites

The observed COVID-19 incidence rates and SARS-CoV-2 wastewater loads varied across the 20 North Carolina sewersheds participating in this study (Fig 2). The sites were distributed across North Carolina, covering approximately 20% of the population and about 2% of the land area. There was a wide range in sewershed size, with the largest sewershed, Raleigh, serving 551,534 people at a capacity of 341 ML/day and the smallest sewershed, Newport, serving 3,731 people at a capacity of 5 ML/day (Table 1). During the study period, the number of samples collected per site ranged from 33 (Wilson, Buncombe, Roanoke Rapids, and Winston-Salem) to 83 (Beaufort). SARS-CoV-2 RNA was detectable in 74% of the 1,129 wastewater

Fig 2. Time series of SARS-CoV-2 wastewater loads (log GC pppd) and COVID-19 incidence (cases/100k) for each of the 20 sites from January through October 2021. Note: COVID-19 incidence is shown as a 7-day rolling average with the blue line. SARS-CoV-2 wastewater loads are depicted with the orange dots and a LOESS curve was fitted to these values, depicted by the orange line (span = 0.3).

https://doi.org/10.1371/journal.pwat.0000140.g002

samples across all 20 sites. Sewersheds with larger populations tended to have higher detection frequencies, with 50% of all the non-detects occurring at the three smallest sites with populations under 5,000 people. The lowest median daily load was 1.3 x 10^5 GC pppd, observed at Newport, while the highest median daily load of 1.6 x 10^7 GC pppd was observed at Charlotte 3 (S2 Table). There were a total of 122,444 COVID-19 cases reported across all 20 sites during the study period, with the median daily incidence rate ranging from 0 cases/100,000 people (Newport, Pittsboro) to 42 cases/100,000 people (Beaufort). Comparable to the wastewater loads, the three smallest sewersheds accounted for almost 75% of the observed days with zero reported COVID-19 cases.

The maximum daily population normalized loads (henceforth referred to simply as loads) for each site ranged from 4.7×10^6 GC pppd to 4.3×10^8 GC pppd, with most of these values occurring in January or late August/early September, during which peaks in COVID-19 cases were also observed with daily incidence rates as high as 235 cases/100,000 people (Fig 2). For the 10 sites that were sampled for the entire 10-month period, there was also a noticeable lull during the period of May to July 2021 for both the wastewater loads and cases. All but one sewershed had significant positive correlations between the wastewater loads and cases observed on the same day, with the significant Spearman's coefficients ranging from $\rho = 0.34$ to $\rho = 0.85$, with a median of $\rho = 0.72$ (S2 Table). The smallest sewershed (Newport) had a non-significant correlation with a coefficient of $\rho = 0.21$ and p-value of 0.09.

Detrending reveals short-term associations

Applying each detrending smoothing range ($T = \infty$, 16, 8, 4 and 2 weeks) across temporal offsets (τ = -7 to τ = +7 days) allowed us to evaluate the lead/lag relationship between the

detrended wastewater and case residuals at progressively finer time scales. Correlation plots similar to Fig 1e were generated for all 20 sewersheds (S2–S21 Figs), and the proposed criteria were used to identify the optimal detrending smoothing range for each site, which was defined as the shortest kernel smoothing range that revealed an identifiable lead or lag (Fig 3). For $T = \infty$ weeks (equivalent to no detrending), lead/lag relationships were inconclusive at eighteen of the 20 sites due to statistically significant correlation coefficients at all temporal offsets. This indicates that detrending was needed to reveal the fine time scale fluctuations required for a lead/lag analysis. Beaufort and Pittsboro were the only sewersheds for which the $T = \infty$ weeks range was optimal for identifying the lead/lag relationship; the detrended wastewater and case residuals were no longer significantly correlated over any 2-day span of temporal offsets using shorter detrending smoothing ranges.

Of the remaining sewersheds, one site had an optimal detrending smoothing range of $T = 16$ weeks, eight sites had an optimal detrending smoothing range of $T = 8$ weeks, and four sites had an optimal detrending smoothing range of $T = 4$ weeks (Fig 3). As a general pattern, the detrending smoothing ranges greater than the identified optimal T either had significant positive correlations at all temporal offsets, such that no lead/lag pattern was identifiable, or additional detrending allowed us to detect fluctuations over a shorter duration while still meeting all the proposed criteria. Conversely, too much of the trend was removed when using values for T smaller than the optimal detrending smoothing range, such that the detrended residuals were no longer significantly correlated for any span of contiguous temporal offsets. With detrending, five of the 20 sewersheds (Wilson, Laurinburg, Marion, MSD of Buncombe

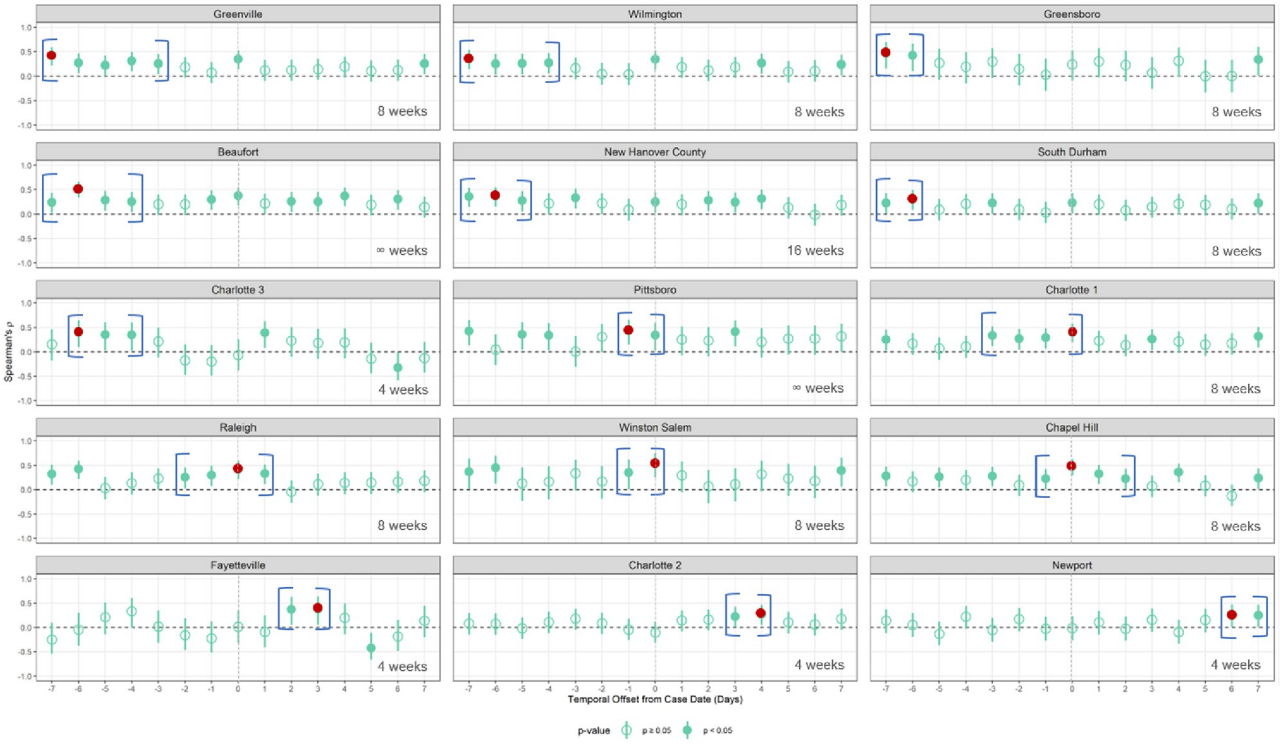

Fig 3. Plots of Spearman's correlation coefficient versus temporal offset at the optimal detrending smoothing range for each of the 15 conclusive sites, ordered from longest lead to longest lag. The highest correlation value is colored in red, the identified lead or lag span is represented with brackets, and the optimal smoothing range is listed in the bottom right corner of each plot. Note: The lead/lag relationship was inconclusive for Wilson, Laurinburg, Marion, MSD of Buncombe County, and Roanoke Rapids, and these plots are therefore not presented.

https://doi.org/10.1371/journal.pwat.0000140.g003

County, and Roanoke Rapids) were deemed inconclusive as none of the detrending smoothing ranges revealed an identifiable lead or lag between the detrended wastewater loads and cases, according to the proposed criteria (Supporting Information). Thus, with this approach, we were able to reduce the number of inconclusive sewersheds from 18 sites (90%) to 5 sites (25%). We identified two reasons for this: 1) the span of consecutive lead/lag values was longer than 7 days for larger *T* values (not identifiable) and shorter than 2 days at smaller T values (not persistent), or 2) the longest range of consecutive lead/lag values did not include the maximum correlation coefficient (not predictive). The inconclusive nature of the lead/lag relationship in these sewersheds may be linked to the short sampling duration or the small size of the sewershed as all five sites had data for only half of the study duration and all but Buncombe County were among the smallest sewersheds.

Detrended wastewater loads were temporally leading detrended COVID-19 cases in 11 of the 15 sewersheds where we were able to identify optimal detrending smoothing ranges (Fig 4). For these sites, the highest correlation was observed for wastewater loads sampled at a median lead time of 6 days before the cases were reported, with a contiguous span of elevated correlations lasting a median of 3 days. At four sewersheds, the correlation between detrended wastewater loads and detrended cases was greatest when the detrended wastewater loads were lagging, with the highest correlation identified at a median of 3.5 days after the cases were reported and a median contiguous span of elevated correlations of 2 days. Although the smaller sewersheds were more likely to be inconclusive, size did not seem to influence the lead/lag relationship at the 15 conclusive sites, with about the same proportion of leading vs

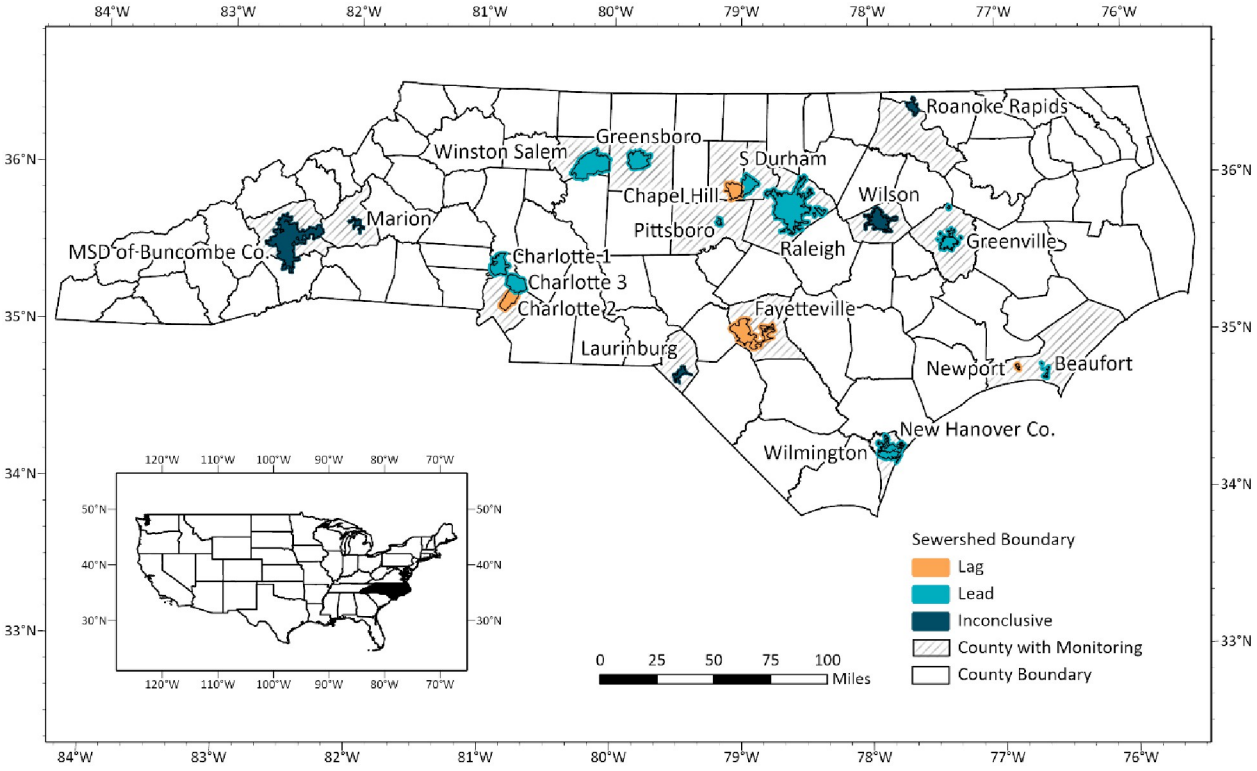

Fig 4. Locations of NC wastewater monitoring network sewersheds participating between January and October 2021. In 11 sewersheds, detrended wastewater leads cases (lead), in 4 sewersheds detrended wastewater lags cases (lag) and in 5 sewersheds results were inconclusive. US state boundaries and North Carolina County boundaries: https://www.nconemap.gov

https://doi.org/10.1371/journal.pwat.0000140.g004

lagging between groups of the smallest and largest sewersheds. However, the optimal detrending smoothing range seemed to be related to the lead/lag relationship, as 64% (7/11) of the leading sewersheds had an optimal detrending smoothing range of $T = 8$ weeks and 75% (3/4) of the lagging sewersheds had an optimal detrending smoothing range of $T = 4$ weeks, suggesting that it may be easier to identify detrended wastewater loads lagging detrended COVID-19 cases at shorter detrending time scales. The optimal smoothing range, relationship, span, and temporal offset with the highest correlation identified for each sewershed are summarized in S3 Table.

Discussion

Wastewater surveillance emerged during the pandemic as a potential leading indicator of COVID-19 infection trends in the community. Although previous research analyzed the overall correlation between SARS-CoV-2 wastewater loads and clinical cases, this analysis used kernel detrending to characterize short-term relationships and identify sub-trends. By detrending wastewater viral loads and cases in the sewershed using various kernel smoothing ranges, we were able to characterize lead/lag relationships at 15 of the 20 North Carolina sewersheds assessed using a set of reproducible criteria, reducing the proportion of inconclusive results from 90% without detrending to 25% using the optimal detrending smoothing range. Furthermore, we found that detrended wastewater loads temporally led detrended cases at almost three times as many sewersheds (N = 11) as sewersheds where detrended wastewater loads lagged detrended cases (N = 4), further highlighting the utility of wastewater as a leading indicator of COVID-19 cases in North Carolina. The optimal detrending kernel smoothing range that removed long-scale pandemic trends while retaining sufficient temporal correlation to identify lead/lag relationships was in the range of 4 to 8 weeks at 12 of the 15 sites with conclusive relationships. Because detrending with a given smoothing range retains only the variation in the observations at time scales shorter than the corresponding timeframe, this finding suggests that this approach is ideal for identifying the leading or lagging nature of wastewater and case trends in most sewersheds experiencing a sustained period of increasing SARS-CoV-2 infection rates lasting at least 4 to 8 weeks. A sustained 4 to 8 weeks increase in COVID-19 incidence corresponding to the emergence of the Delta variant (B.1.617.2) in late July 2021 was observed in wastewater loads at 19 of the 20 study sites, further supporting the wider relevance of this range during the study period. However, due to onboarding schedules, some sewersheds were only sampled for half of the study period, and the shorter sampling history appeared related to inconclusive results at these sites.

A strength of our study is that we performed a lead/lag analysis across a wide-range of WWTP systems, including both rural and urban municipal systems serving sewershed populations ranging from under 4,000 to 550,000 people [16,24,38–40]. Although we identified a leading relationship in the majority of North Carolina sewersheds, those within the same county or in adjacent counties did not always exhibit the same lead/lag relationship nor have the same optimal detrending smoothing range (Fig 4). For example, we found that detrended wastewater loads led detrended cases at Charlotte 1 and Charlotte 3 but lagged detrended cases at Charlotte 2 (Fig 4, S2 Table). Wastewater led cases in both the Wilmington sewershed and the sewershed encompassing surrounding areas of New Hanover County, but the optimal detrending smoothing range was 8 weeks for the city and 16 weeks in the county, which covers a larger land area but serves fewer people (Table 1). Differences in the temporal relationship or optimal smoothing range at each sewershed could be due to conditions at a given site: virus loads measured in wastewater can be impacted by sewer network infrastructure age, sewer residence time, or weather [39,41,42], and clinical surveillance is subject to underreporting due to

testing access, home test usage, or fluctuations in populations from tourists and commuters [43]. To minimize the potential impact of testing behavior on the evaluation of relationships between SARS-CoV-2 loads and COVID-19 cases presented in this work, we chose to perform the analysis for a period ending prior to November 2021, when clinical testing penetration was still relatively high and home testing was not yet widely used in North Carolina communities.

Given that site-specific conditions can influence wastewater results, public health agencies leading wastewater surveillance programs in their jurisdictions may want to validate their wastewater data against other foundational COVID-19 metrics to determine how wastewater surveillance fits into their larger surveillance strategies. For states or jurisdictions less familiar with wastewater data, a lead/lag analysis between wastewater loads and reported cases would be a useful method to help understand the temporal relationship between wastewater-based pathogen and other decision-making metrics. Our method can be employed by public health agencies participating in CDC NWSS across the United States by using an R Markdown document that applies set criteria to identify the leading or lagging relationships between wastewater and reported cases [37]. As counts of reported cases become less reliable over time due to an increase in non-reportable results from at-home-testing kits, as well as an overall reduction in PCR-based, reportable, COVID-19 clinical testing, this method can be adapted to utilize surveillance metrics besides cases, including hospitalizations, emergency department visits (syndromic surveillance data), or mortality [17].

Results from our analysis characterizing the shortest time ranges at which wastewater loads are associated with cases have been formative in elevating wastewater as a reliable metric for tracking trends in North Carolina, not only to anticipate the start of long-term cycles (such as the start of elevated rates in winter), but also for short duration fluctuations within any given long-term cycle. The leading nature of wastewater-based COVID-19 findings at most sites provides the foundation and rationale for including wastewater loads as an early warning metric alongside reported cases, emergency department visits, and hospitalizations, which are highlighted on statewide data surveillance dashboards such as the NCDHHS COVID-19 dashboard (https://covid19.ncdhhs.gov/dashboard/wastewater-monitoring).

In under two years, COVID-19 wastewater surveillance in the United States expanded from 8 pilot state health agencies participating in the CDC National Wastewater Surveillance System in 2020 to 50 states, 5 cities, 3 territories, and 7 tribes participating in 2023 [44]. Similarly, the global portal expanded to cover 72 countries, reporting for 4,648 sites, indicating widespread use of wastewater surveillance data [45]. With the explosive growth in both the academic literature on, and implementation of, wastewater surveillance programs globally, public health professionals developed a wide range of approaches to utilizing wastewater data for decision making. Our method shows how detrended wastewater loads can predict finer scale fluctuations in detrended cases, which can allow public health officials to respond more locally and timely when COVID-19 burden, or other disease burden as wastewater surveillance expands to new targets, is increasing at levels greater than the baseline trend. Examples of mitigation strategies that can be deployed at local levels and for short durations, while being complementary to long lasting statewide measures, may include the following: (a) officials could quickly alert local hospitals about a potential increase in cases above the statewide trend and provide recommendations to community leaders to implement short-duration restrictions, such as limiting indoor gatherings and reducing business capacity [46]; (b) jurisdictions could mobilize pop-up testing and take steps to increase vaccination in the community [47]; (c) increasing public health communications regarding masking, handwashing, vaccination, and social distancing to help contain the spread of the virus; and d) interacting with local public health officials and hospital administrators to indicate periods of higher ICU bed, PPE, and medical staffing needs. This has already been observed during a large sport fishing tournament that

took place in a small coastal North Carolina sewershed where NCDHHS notified local health department and city officials of an increase in wastewater viral load. In response to this increase, local health department and city officials reinforced recommended mitigation strategies outlined in the Governor's Executive order to the event leadership, like additional handwashing stations and frequent disinfection of high touch surfaces (Nina Oliver, Carteret County Health Director, personal communication, June 21–22 2021 & February 6, 2023). Local notices were also used to encourage the surrounding community to take precautions through vaccinations, masking, social distancing, and frequent handwashing [48]. Immediately following the event, county and city officials met routinely to review wastewater, as well as other COVID-19 metrics, and to ensure levels were decreasing (Nina Oliver, personal communication, February 6, 2023). Additional program evaluation is needed to understand the efficacy of these public health actions; evaluation is ongoing in NC.

As public health officials and the scientific community continue to rely on wastewater surveillance both for large-scale pandemic decision-making and localized action as described here, there is a growing need for increasing equitable access to wastewater services, particularly in cases of municipal underbounding, and for investing in substantial infrastructure improvements. This is especially important in jurisdictions like North Carolina, where half of households rely on private septic and package treatment plants [49]. In some cases, racial disparities in access to and disproportionate exclusion from municipal water and sewer service have been documented [49–51]. In other areas, distance, lack of gradient, and groundwater height play a role in decisions to use centralized versus decentralized waste treatment systems. For wastewater to continue to be useful for disease tracking and public health decision-making beyond COVID-19, additional resources are needed to achieve equitable access to centralized wastewater treatment where it is desired and environmentally relevant. In other rural areas where this is not the case, we need to improve our technical capabilities to characterize decentralized waste systems.

Supporting information

S1 Fig. Overview of sample collection and processing methods.
(TIF)

S2 Fig. Beaufort sewershed COVID-19 incidence rate cross-correlation plots with wastewater viral load for smoothing ranges of ∞, 16, 8, 4, and 2 weeks.
(TIF)

S3 Fig. Chapel Hill sewershed COVID-19 incidence rate cross-correlation plots with wastewater viral load for smoothing ranges of ∞, 16, 8, 4, and 2 weeks.
(TIF)

S4 Fig. Charlotte 1 sewershed COVID-19 incidence rate cross-correlation plots with wastewater viral load for smoothing ranges of ∞, 16, 8, 4, and 2 weeks.
(TIF)

S5 Fig. Charlotte 2 sewershed COVID-19 incidence rate cross-correlation plots with wastewater viral load for smoothing ranges of ∞, 16, 8, 4, and 2 weeks.
(TIF)

S6 Fig. Charlotte 3 sewershed COVID-19 incidence rate cross-correlation plots with wastewater viral load for smoothing ranges of ∞, 16, 8, 4, and 2 weeks.
(TIF)

S7 Fig. Fayetteville sewershed COVID-19 incidence rate cross-correlation plots with wastewater viral load for smoothing ranges of ∞, 16, 8, 4, and 2 weeks.
(TIF)

S8 Fig. Greensboro sewershed COVID-19 incidence rate cross-correlation plots with wastewater viral load for smoothing ranges of ∞, 16, 8, 4, and 2 weeks.
(TIF)

S9 Fig. Greenville sewershed COVID-19 incidence rate cross-correlation plots with wastewater viral load for smoothing ranges of ∞, 16, 8, 4, and 2 weeks.
(TIF)

S10 Fig. Laurinburg sewershed COVID-19 incidence rate cross-correlation plots with wastewater viral load for smoothing ranges of ∞, 16, 8, 4, and 2 weeks.
(TIF)

S11 Fig. Marion sewershed COVID-19 incidence rate cross-correlation plots with wastewater viral load for smoothing ranges of ∞, 16, 8, 4, and 2 weeks.
(TIF)

S12 Fig. MSD of Buncombe County sewershed COVID-19 incidence rate cross-correlation plots with wastewater viral load for smoothing ranges of ∞, 16, 8, 4, and 2 weeks.
(TIF)

S13 Fig. New Hanover County sewershed COVID-19 incidence rate cross-correlation plots with wastewater viral load for smoothing ranges of ∞, 16, 8, 4, and 2 weeks.
(TIF)

S14 Fig. Newport sewershed COVID-19 incidence rate cross-correlation plots with wastewater viral load for smoothing ranges of ∞, 16, 8, 4, and 2 weeks.
(TIF)

S15 Fig. Pittsboro sewershed COVID-19 incidence rate cross-correlation plots with wastewater viral load for smoothing ranges of ∞, 16, 8, 4, and 2 weeks.
(TIF)

S16 Fig. Raleigh sewershed COVID-19 incidence rate cross-correlation plots with wastewater viral load for smoothing ranges of ∞, 16, 8, 4, and 2 weeks.
(TIF)

S17 Fig. Roanoke Rapids sewershed COVID-19 incidence rate cross-correlation plots with wastewater viral load for smoothing ranges of ∞, 16, 8, 4, and 2 weeks.
(TIF)

S18 Fig. South Durham sewershed COVID-19 incidence rate cross-correlation plots with wastewater viral load for smoothing ranges of ∞, 16, 8, 4, and 2 weeks.
(TIF)

S19 Fig. Wilmington sewershed COVID-19 incidence rate cross-correlation plots with wastewater viral load for smoothing ranges of ∞, 16, 8, 4, and 2 weeks.
(TIF)

S20 Fig. Wilson sewershed COVID-19 incidence rate cross-correlation plots with wastewater viral load for smoothing ranges of ∞, 16, 8, 4, and 2 weeks.
(TIF)

S21 Fig. Winston-Salem sewershed COVID-19 incidence rate cross-correlation plots with wastewater viral load for smoothing ranges of ∞, 16, 8, 4, and 2 weeks.
(TIF)

S1 Table. ddPCR assay primer and probe sequences.
(DOCX)

S2 Table. Summary statistics by sewershed of COVID-19 incidence rates, wastewater SARS-CoV-2 loads, and their correlation.
(DOCX)

S3 Table. Summary of the optimal smoothing range, timing relationship of wastewater to cases, span of temporal offsets significant for the timing relationship between wastewater and cases, and the temporal offset with the highest correlation identified according to the proposed criteria for each sewershed.
(DOCX)

S1 Text. Supporting information: Text with associated references.
(DOCX)

S1 Code. Exponential kernel smoothing R Function.
(TIF)

Acknowledgments

We gratefully acknowledge Jane Hoppin, and other UNC system researchers who were involved building the 2020 NC Wastewater Pathogen Research Network (NC WW Path); these partners conducted integral research to inform and launch the state surveillance system (NC Wastewater Monitoring Network) in January 2021. We also wish to thank Nina Oliver, the Carteret County Health Director, as well as local health departments, county and city officials, and wastewater utilities participating in wastewater monitoring across NC. We appreciate your tireless work to protect the public's health.

Author Contributions

Conceptualization: Kelly Hoffman, David Holcomb, Stacie Reckling, Thomas Clerkin, Virginia T. Guidry, Lawrence Engel, Marc Serre, Ariel Christensen.

Data curation: Stacie Reckling, Denene Blackwood, Angela Harris, Rachel Noble, Ariel Christensen.

Formal analysis: Kelly Hoffman, David Holcomb, Thomas Clerkin, Denene Blackwood, Rachelle Beattie, Angela Harris, Ariel Christensen.

Investigation: Kelly Hoffman, David Holcomb, Stacie Reckling, Thomas Clerkin, Rachel Noble, Ariel Christensen.

Methodology: David Holcomb, Stacie Reckling, Denene Blackwood, Lawrence Engel, Marc Serre, Ariel Christensen.

Project administration: Marc Serre, Ariel Christensen.

Supervision: Stacie Reckling, Angela Harris, Rachel Noble, Virginia T. Guidry, Lawrence Engel, Marc Serre, Ariel Christensen.

Validation: Kelly Hoffman, David Holcomb, Stacie Reckling, Thomas Clerkin, Helena Mitasova, Mariya Munir, Steven Berkowitz, Virginia T. Guidry, Marc Serre, Ariel Christensen.

Visualization: Kelly Hoffman, David Holcomb, Stacie Reckling, Lawrence Engel, Marc Serre, Ariel Christensen.

Writing – original draft: Kelly Hoffman, David Holcomb, Stacie Reckling, Thomas Clerkin, Denene Blackwood, Rachelle Beattie, Francis de los Reyes, Angela Harris, Rachel Noble, Lawrence Engel, Marc Serre, Ariel Christensen.

Writing – review & editing: Kelly Hoffman, David Holcomb, Stacie Reckling, Thomas Clerkin, Denene Blackwood, Rachelle Beattie, Francis de los Reyes, Angela Harris, Helena Mitasova, Nadine Kotlarz, Jill Stewart, Jacob Kazenelson, Lawrence Cahoon, Arthur Frampton, Mariya Munir, Allison Lee, Steven Berkowitz, Rachel Noble, Virginia T. Guidry, Lawrence Engel, Marc Serre, Ariel Christensen.

References

1. NCDHHS. North Carolina COVID-19 Dashboard. In: North Carolina Department of Health and Human Services [Internet]. 2023 [cited 12 Sep 2022]. https://covid19.ncdhhs.gov/dashboard.
2. NCDHHS. North Carolina Identifies First Case of COVID-19. North Carolina Department of Health and Human Services; 2020. https://www.ncdhhs.gov/news/press-releases/2020/03/03/north-carolina-identifies-first-case-covid-19.
3. Alwan NA. Surveillance is underestimating the burden of the COVID-19 pandemic. The Lancet. 2020; 396: e24. https://doi.org/10.1016/S0140-6736(20)31823-7 PMID: 32861312
4. Wu F, Xiao A, Zhang J, Moniz K, Endo N, Armas F, et al. SARS-CoV-2 RNA concentrations in wastewater foreshadow dynamics and clinical presentation of new COVID-19 cases. Science of The Total Environment. 2022; 805: 150121. https://doi.org/10.1016/j.scitotenv.2021.150121 PMID: 34534872
5. Xiao A, Wu F, Bushman M, Zhang J, Imakaev M, Chai PR, et al. Metrics to relate COVID-19 wastewater data to clinical testing dynamics. Water Res. 2022; 212: 118070. https://doi.org/10.1016/j.watres.2022.118070 PMID: 35101695
6. Brandt K, Goel V, Keeler C, Bell GJ, Aiello AE, Corbie-Smith G, et al. SARS-CoV-2 testing in North Carolina: Racial, ethnic, and geographic disparities. Health & Place. 2021; 69: 102576. https://doi.org/10.1016/j.healthplace.2021.102576 PMID: 33915376
7. Jacobson M, Chang TY, Shah M, Pramanik R, Shah SB. Racial and Ethnic Disparities in SARS-CoV-2 Testing and COVID-19 Outcomes in a Medicaid Managed Care Cohort. American Journal of Preventive Medicine. 2021; 61: 644–651. https://doi.org/10.1016/j.amepre.2021.05.015 PMID: 34412946
8. Lieberman-Cribbin W, Tuminello S, Flores RM, Taioli E. Disparities in COVID-19 Testing and Positivity in New York City. American Journal of Preventive Medicine. 2020; 59: 326–332. https://doi.org/10.1016/j.amepre.2020.06.005 PMID: 32703702
9. Bivins A, North D, Ahmad A, Ahmed W, Alm E, Been F, et al. Wastewater-Based Epidemiology: Global Collaborative to Maximize Contributions in the Fight Against COVID-19. Environmental Science & Technology. 2020; acs.est.0c02388. https://doi.org/10.1021/acs.est.0c02388 PMID: 32530639
10. Barua VB, Juel MAI, Blackwood AD, Clerkin T, Ciesielski M, Sorinolu AJ, et al. Tracking the temporal variation of COVID-19 surges through wastewater-based epidemiology during the peak of the pandemic: A six-month long study in Charlotte, North Carolina. Science of The Total Environment. 2022; 814: 152503. https://doi.org/10.1016/j.scitotenv.2021.152503 PMID: 34954186
11. Murakami M, Hata A, Honda R, Watanabe T. Letter to the Editor: Wastewater-Based Epidemiology Can Overcome Representativeness and Stigma Issues Related to COVID-19. Environ Sci Technol. 2020; acs.est.0c02172. https://doi.org/10.1021/acs.est.0c02172 PMID: 32323978
12. Crank K, Chen W, Bivins A, Lowry S, Bibby K. Contribution of SARS-CoV-2 RNA shedding routes to RNA loads in wastewater. Science of The Total Environment. 2021; 150376. https://doi.org/10.1016/j.scitotenv.2021.150376 PMID: 34610564
13. Natarajan A, Zlitni S, Brooks EF, Vance SE, Dahlen A, Hedlin H, et al. Gastrointestinal symptoms and fecal shedding of SARS-CoV-2 RNA suggest prolonged gastrointestinal infection. Med. 2022; 3: 371–387.e9. https://doi.org/10.1016/j.medj.2022.04.001 PMID: 35434682
14. Schmitz BW, Innes GK, Prasek SM, Betancourt WQ, Stark ER, Foster AR, et al. Enumerating asymptomatic COVID-19 cases and estimating SARS-CoV-2 fecal shedding rates via wastewater-based

epidemiology. Science of The Total Environment. 2021; 801: 149794. https://doi.org/10.1016/j.scitotenv.2021.149794 PMID: 34467933

15. Fernandez-Cassi X, Scheidegger A, Bänziger C, Cariti F, Tuñas Corzon A, Ganesanandamoorthy P, et al. Wastewater monitoring outperforms case numbers as a tool to track COVID-19 incidence dynamics when test positivity rates are high. Water Research. 2021; 200: 117252. https://doi.org/10.1016/j.watres.2021.117252 PMID: 34048984

16. Fitzgerald SF, Rossi G, Low AS, McAteer SP, O'Keefe B, Findlay D, et al. Site Specific Relationships between COVID-19 Cases and SARS-CoV-2 Viral Load in Wastewater Treatment Plant Influent. Environmental Science & Technology. 2021; 55: 15276–15286. https://doi.org/10.1021/acs.est.1c05029 PMID: 34738785

17. Kotlarz N, Holcomb D, Pasha T, Reckling S, Kays J, Lai Y, et al. Timing and trends for municipal wastewater, clinically confirmed case, and syndromic case surveillance of COVID-19 in Raleigh, North Carolina, USA. American Journal of Public Health. 2023; 113: 79–88. https://doi.org/10.2105/AJPH.2022.307108 PMID: 36356280

18. Weidhaas J, Aanderud ZT, Roper DK, VanDerslice J, Gaddis EB, Ostermiller J, et al. Correlation of SARS-CoV-2 RNA in wastewater with COVID-19 disease burden in sewersheds. Science of the Total Environment. 2021; 775: 145790. https://doi.org/10.1016/j.scitotenv.2021.145790 PMID: 33618308

19. Graham KE, Loeb SK, Wolfe MK, Catoe D, Sinnott-Armstrong N, Kim S, et al. SARS-CoV-2 RNA in Wastewater Settled Solids Is Associated with COVID-19 Cases in a Large Urban Sewershed. Environmental Science & Technology. 2020; acs.est.0c06191. https://doi.org/10.1021/acs.est.0c06191 PMID: 33283515

20. Omori R, Miura F, Kitajima M. Age-dependent association between SARS-CoV-2 cases reported by passive surveillance and viral load in wastewater. Science of The Total Environment. 2021; 792: 148442. https://doi.org/10.1016/j.scitotenv.2021.148442 PMID: 34147797

21. Peccia J, Zulli A, Brackney DE, Grubaugh ND, Kaplan EH, Casanovas-Massana A, et al. Measurement of SARS-CoV-2 RNA in wastewater tracks community infection dynamics. Nature Biotechnology. 2020; 38: 1164–1167. https://doi.org/10.1038/s41587-020-0684-z PMID: 32948856

22. Zhao L, Zou Y, Li Y, Miyani B, Spooner M, Gentry Z, et al. Five-week warning of COVID-19 peaks prior to the Omicron surge in Detroit, Michigan using wastewater surveillance. Science of The Total Environment. 2022; 844: 157040. https://doi.org/10.1016/j.scitotenv.2022.157040 PMID: 35779714

23. Grube A. M., Coleman C. K., LaMontagne C. D., Miller M. E., Kothegal N. P., Holcomb D. A., et al. (2023). Detection of SARS-CoV-2 RNA in wastewater and comparison to COVID-19 cases in two sewersheds, North Carolina, USA. The Science of the total environment, 858(Pt 3), 159996. https://doi.org/10.1016/j.scitotenv.2022.159996 PMID: 36356771

24. Keshaviah A, Huff I, Hu XC, Guidry V, Christensen A, Berkowitz S, et al. Separating Signal from Noise in Wastewater Data: An Algorithm to Identify Community-Level COVID-19 Surges. Proceedings of the National Academy of Sciences. 2023. https://doi.org/10.1073/pnas.2216021120 PMID: 37490532

25. Bibby K, Bivins A, Wu Z, North D. Making waves: Plausible lead time for wastewater based epidemiology as an early warning system for COVID-19. Water Research. 2021; 202: 117438. https://doi.org/10.1016/j.watres.2021.117438 PMID: 34333296

26. Olesen SW, Imakaev M, Duvallet C. Making waves: Defining the lead time of wastewater-based epidemiology for COVID-19. Water Research. 2021; 202: 117433. https://doi.org/10.1016/j.watres.2021.117433 PMID: 34304074

27. Akita Y, Carter G, Serre ML. Spatiotemporal Nonattainment Assessment of Surface Water Tetrachloroethylene in New Jersey. Journal of Environmental Quality. 2007; 36: 508–520. https://doi.org/10.2134/jeq2005.0426 PMID: 17332255

28. Cleland SE, West JJ, Jia Y, Reid S, Raffuse S, O'Neill S, et al. Estimating Wildfire Smoke Concentrations During the October 2017 California Fires Through BME Space/Time Data Fusion of Observed, Modeled, and Satellite-Derived PM2.5. Environmental science & technology. 2020; 54: 13439. https://doi.org/10.1021/acs.est.0c03761 PMID: 33064454

29. de Nazelle A, Arunachalam S, Serre ML. Bayesian Maximum Entropy Integration of Ozone Observations and Model Predictions: An Application for Attainment Demonstration in North Carolina. Environmental science & technology. 2010; 44: 5707–5713. https://doi.org/10.1021/es100228w PMID: 20590110

30. Jat P, Serre ML. Bayesian Maximum Entropy Space/time Estimation of Surface Water Chloride in Maryland Using River Distances. Environmental Pollution. 2016; 219: 1148–1155. https://doi.org/10.1016/j.envpol.2016.09.020 PMID: 27616646

31. Rudolph JE, Cole SR, Edwards JK, Whitsel EA, Serre ML, Richardson DB. Estimating Associations Between Annual Concentrations of Particulate Matter and Mortality in the United States, Using Data Linkage and Bayesian Maximum Entropy. Epidemiology. 2022; 33: 157–166. https://doi.org/10.1097/EDE.0000000000001447 PMID: 34816807

32. NC Wastewater Pathogen Research Network. Tracking SARS-CoV-2 in the Wastewater Across a Range of North Carolina Municipalities: Final Report. North Carolina Policy Collaboratory; 2021 Feb. https://collaboratory.unc.edu/wp-content/uploads/sites/476/2021/02/tracking-sars-cov-2-in-the-wastewater-across-a-range-of-north-carolina-municipalities-report.pdf.

33. Beattie RE, Blackwood AD, Clerkin T, Dinga C, Noble RT. Evaluating the impact of sample storage, handling, and technical ability on the decay and recovery of SARS-CoV-2 in wastewater. PLOS ONE. 2022; 17: 1–16. https://doi.org/10.1371/journal.pone.0270659 PMID: 35749532

34. Borchardt MA, Boehm AB, Salit M, Spencer SK, Wigginton KR, Noble RT. The Environmental Microbiology Minimum Information (EMMI) Guidelines: qPCR and dPCR Quality and Reporting for Environmental Microbiology. Environmental Science & Technology. 2021. https://doi.org/10.1021/acs.est.1c01767 PMID: 34286966

35. Lu X, Wang L, Sakthivel SK, Whitaker B, Murray J, Kamili S, et al. US CDC Real-Time Reverse Transcription PCR Panel for Detection of Severe Acute Respiratory Syndrome Coronavirus 2. Emerging Infectious Diseases. 2020; 26: 1654–1665. https://doi.org/10.3201/eid2608.201246 PMID: 32396505

36. R Core Team. R: A Language and Environment for Statistical Computing. R Foundation for Statistical Computing, Vienna, Austria. 2021. https://www.R-project.org/.

37. rmarkdown: Dynamic Documents for R. RStudio; 2023. https://github.com/rstudio/rmarkdown.

38. Feng S, Roguet A, McClary-Gutierrez JS, Newton RJ, Kloczko N, Meiman JG, et al. Evaluation of Sampling, Analysis, and Normalization Methods for SARS-CoV-2 Concentrations in Wastewater to Assess COVID-19 Burdens in Wisconsin Communities. ACS ES&T Water. 2021; 1: 1955–1965. https://doi.org/10.1021/acsestwater.1c00160

39. Hoar C, Chauvin F, Clare A, McGibbon H, Castro E, Patinella S, et al. Monitoring SARS-CoV-2 in wastewater during New York City's second wave of COVID-19: sewershed-level trends and relationships to publicly available clinical testing data. Environmental Science: Water Research & Technology. 2022; 8: 1021–1035. https://doi.org/10.1039/D1EW00747E

40. Holm RH, Mukherjee A, Rai JP, Yeager RA, Talley D, Rai SN, et al. SARS-CoV-2 RNA abundance in wastewater as a function of distinct urban sewershed size. Environmental Science: Water Research & Technology. 2022; https://doi.org/10.1039/D1EW00672J

41. Guo Y, Sivakumar M, Jiang G. Decay of four enteric pathogens and implications to wastewater-based epidemiology: Effects of temperature and wastewater dilutions. Science of The Total Environment. 2022; 819: 152000. https://doi.org/10.1016/j.scitotenv.2021.152000 PMID: 34843787

42. Zhu Y, Oishi W, Maruo C, Saito M, Chen R, Kitajima M, et al. Early warning of COVID-19 via wastewater-based epidemiology: potential and bottlenecks. Science of The Total Environment. 2021; 767: 145124. https://doi.org/10.1016/j.scitotenv.2021.145124 PMID: 33548842

43. Sharara N, Endo N, Duvallet C, Ghaeli N, Matus M, Heussner J, et al. Wastewater network infrastructure in public health: Applications and learnings from the COVID-19 pandemic. PLOS Global Public Health. 2021; 1: e0000061. https://doi.org/10.1371/journal.pgph.0000061 PMID: 34927170

44. CDC. Wastewater Surveillance: A New Frontier for Public Health. In: Centers for Disease Control and Prevention [Internet]. 19 Jul 2022 [cited 12 Sep 2022]. https://www.cdc.gov/amd/whats-new/wastewater-surveillance.html.

45. Naughton CC, Roman, Fernando A J, Alvarado AGF, Tariqi AQ, Deeming MA, Kadonsky KF, et al. Show us the data: global COVID-19 wastewater monitoring efforts, equity, and gaps. FEMS Microbes. 2023; 4. https://doi.org/10.1093/femsmc/xtad003 PMID: 37333436

46. Garcia K, Christensen A, Reckling S, Berkowitz S, Guidry V. Local Partnership Building—NC Wastewater Monitoring Program for SARS-CoV-2. Council of State and Territorial Epidemiologists (CSTE) Annual Conference; 2022 Jun; Louisville, KY.

47. Hopkins L, Ensor KB, Stadler L, et al. Public Health Interventions Guided by Houston's Wastewater Surveillance Program During the COVID-19 Pandemic. Public Health Reports. 2023; 0(0). https://doi.org/10.1177/00333549231185625 PMID: 37503606

48. Johnson R, Oliver N. COVID-19 Monitoring Detects Elevated Levels of COVID-19 in Wastewater. Town of Beaufort, Carteret County Health Department, North Carolina Department of Health and Human Services; 2021. https://www.beaufortnc.org/sites/default/files/fileattachments/public_utilities/page/10091/wastewater_joint_release_.pdf.

49. Leker HG, Gibson JM. Relationship between race and community water and sewer service in North Carolina, USA. PLOS ONE. 2018; 13: e0193225. https://doi.org/10.1371/journal.pone.0193225 PMID: 29561859

50. MacDonald Gibson J, DeFelice N, Sebastian D, Leker H. Racial Disparities in Access to Community Water Supply Service in Wake County, North Carolina. American Journal of Public Health. 2014; 104: e45. https://doi.org/10.2105/AJPH.2014.10412e45.1

51. Marsh B, Parnell A, Joyner A. Institutionalization of Racial Inequality in Local Political Geographies. Urban Geography. 2010; 31: 691–709. https://doi.org/10.2747/0272-3638.31.5.691

Supporting Information:

Using Detrending to Assess SARS-CoV-2 Wastewater Loads as a Leading Indicator of Fluctuations in COVID-19 Cases at Fine Temporal Scales: Correlations Across Twenty Sewersheds in North Carolina

Kelly Hoffman (co-first author)[1], David Holcomb (co-first author)[1,2], Stacie Reckling[3,4], Thomas Clerkin[5], Denene Blackwood[5], Rachelle Beattie[5], Francis de los Reyes[6], Angela Harris[6], Helena Mitasova[4,7], Nadine Kotlarz[8], Jill Stewart[1], Jacob Kazenelson[9], Lawrence Cahoon[9], Arthur Frampton[9], Mariya Munir[10], Allison Lee[1], Steven Berkowitz[3], Rachel Noble[1,5], Virginia T. Guidry[3], Lawrence Engel[2] (co-senior author), Marc Serre[1] (co-senior author), Ariel Christensen[2,3] (co-senior author)

1. University of North Carolina at Chapel Hill, Department of Environmental Sciences and Engineering, Chapel Hill, NC
2. University of North Carolina at Chapel Hill, Department of Epidemiology, Chapel Hill, NC
3. North Carolina Department of Health and Human Services, Division of Public Health, Raleigh, NC
4. North Carolina State University, Center for Geospatial Analytics, Raleigh, NC
5. University of North Carolina at Chapel Hill, Institute of Marine Sciences, Department of Earth, Marine, and Environmental Sciences, Morehead City, NC
6. North Carolina State University, Department of Civil, Construction, and Environmental Engineering, Raleigh, NC
7. North Carolina State University, Department of Marine, Earth and Atmospheric Sciences, Raleigh, NC
8. North Carolina State University, Department of Biological Sciences, Raleigh, NC
9. University of North Carolina at Wilmington, Department of Biology and Marine Biology, Wilmington, NC
10. University of North Carolina at Charlotte, Department of Civil and Environmental Engineering, Charlotte, NC

This supplement contains 32 pages, 21 figures, and 3 tables.

Table of Contents

S1. Laboratory Methods..... 3

S1.1. Sample Processing and Nucleic Acid Extraction 3

S1.2. SARS-CoV-2 Quantification..... 4

S1.3. ddPCR Data Interpretation and Quality Control 7

S2. Exponential Kernel Smoothing Function 8

S3. Sewershed Wastewater Viral Loads and COVID-19 Incidence..... 9

S4. Site-Specific Cross-Correlations..... 10

S5. Supplementary References 31

S1. Laboratory Methods

S1.1. Sample Processing and Nucleic Acid Extraction

At each wastewater treatment plant (WWTP), 250 mL of 24-hour flow-weighted composite influent wastewater sample was collected twice weekly, stored onsite at 4 °C for up to four days, and shipped once weekly overnight on blue ice to UNC Institute of Marine Sciences (IMS, Morehead City, NC). Upon arrival at IMS, samples were processed and analyzed for SARS-CoV-2 as described previously [1]. Figure S1 presents the sample processing and laboratory analysis workflow that was conducted weekly for each set of samples received at IMS. Briefly, samples and a 250 mL PBS method blank (MB) were heat pasteurized to reach an internal temperature of 56˚C for 30 minutes [2], acidified with 10M HCl to pH 3.5, amended to a final $MgCl_2$ concentration of 25 mM [3], and spiked with approximately 12,525 copies of bovine coronavirus (BCoV; MERECK Animal Health BOVILIS® Coronavirus Calf Vaccine, PBS Animal Health Massillon, OH) as a total processing recovery control. Amended samples were vacuum filtered to dryness in 40 mL volumes through 47 mm, 0.45 µm mixed cellulose ester (MCE) filters (Pall Corp., Port Washington, NY). Filters were placed in 2mL microcentrifuge tubes with sterile forceps and immediately submerged in 1 mL easyMag® Lysis buffer (bioMerieux, Durham, NC) containing 370 copies hepatitis G in Armored RNA® (HepG, Assurgen Austin, TX) as an extraction recovery control. A blank MCE filter was included with each extraction batch to serve as a negative extraction control (NEC). Total nucleic acids were extracted from lysed filters using an automated magnetic particle analyzer (KingFisher™ Flex, Thermo Fisher Scientific, Waltham, MA) and easyMag® NucliSENS ® reagents (bioMerieux, Durham, NC) as described previously [1] and eluted with 100 µL buffer AE (QIAGEN, Germantown, MD).

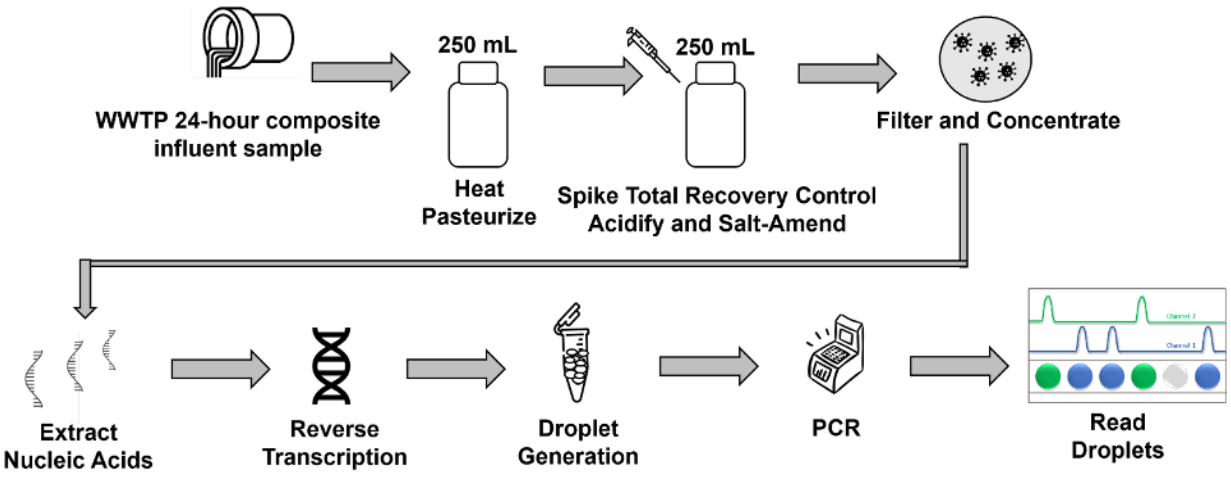

Figure S1. Overview of sample collection and processing methods.

S1.2. SARS-CoV-2 Quantification

The N1 and N2 regions of the SARS-CoV-2 nucleocapsid (N) gene [4] and spiked controls were quantified by two-step reverse transcription droplet digital polymerase chain reaction (RT-ddPCR) as described previously [1]. RT was performed immediately following extraction on 30 µL nucleic acid extract using SuperScript™ IV VILO™ cDNA synthesis mastermix (Thermo Fisher) and ~5 copies of Mouse Normal Lung Total RNA (mouse lung, BioChain, Newark, CA) as an RT efficiency control in a 60 µL reaction volume, corresponding to a 1:2 dilution of the RNA template. Each RT plate included a no RT (NRT) control that excluded reverse transcriptase from the mastermix to confirm only RNA was transcribed. RT was conducted on C1000 Touch™ thermal cycler (BioRad Laboratories, Hercules, CA) with the following cycling conditions: 10 minutes at 25℃ to anneal primers, 10 minutes at 50℃ for the RT reaction, and 5 minutes at 85℃ for enzyme inactivation.

Three sets of duplexed ddPCR assays were performed in duplicate to quantify the two SARS-CoV-2 and four quality control gene targets (Table S1) in 25 µL reaction volumes containing 0.9 nM of each primer, 0.25 nM of each probe, 12.5 µL of ddPCR™ 2X Supermix for Probes (no dUTP, BioRad Laboratories), 5 µL cDNA template, and 140 copies of a haloalkaliphilic archaeon to serve as a PCR

inhibition and efficiency control. Primers and probes were synthesized by LGC Biosearch Technologies (Novato, CA) with the exception of Mouse ACTB (actin, beta) endogenous control (VIC®/MGB Probe, Primer Limited, Life Technologies). After droplet generation in a DG8™ Cartridge (BioRad), droplets were transferred to a 96-well plate for amplification on a C1000 Touch™ thermal cycler (BioRad) with 10 minutes at 95°C for initial denaturation; 40 cycles of 94°C for 30 seconds and annealing at 55°C for 60 seconds; and finished at 98°C for 10 minutes followed by an indefinite hold at 4°C. Positive, negative extraction (NEC), no RT (NRT), and a minimum of 4 no template (NTC) controls consisting of 5 µL nuclease-free water in place of cDNA template were run with every assay [5,6]. Heat inactivated SARS-CoV-2 (strain designation 2019-nCoV/USA-WA1/2020, ATCC Bethesda, MD) served as the positive control for the N1 and N2 assays. PCR efficiency and matrix inhibition was assessed by quantifying the haloalkaliphilic archaeon gyr *a* gene using unpublished primers and probes that were kindly provided by Josh Steele of the Southern California Coastal Water Research Project (SCCWRP). Samples were considered inhibited if the measured gyr *a* concentration was greater than 1 standard deviation different than the spiked control concentration; inhibited samples were diluted 1:2 and subsequently re-quantified.

Table S1. ddPCR assay primer and probe sequences

Target	Purpose	Primer/Probe	Sequence 5'-3'	Nucleotide position	Amplicon length	Reference Accession #
SARS-CoV-2 Nucleocapsid gene N1	Outcome	nCoV N1 Fwd	GACCCCAAAATCAGCGAAAT	28303-28322	73 bp	Lu et al. [4]
		nCoV N1 Rev	TCTGGTTACTGCCAGTTGAATCTG	28374-28351		
		nCoV N1 Probe	FAM-ACCCCGCAT-/ZEN/-TACGTTTGGTGGACC-3IABkFQ	28325-28348		MN908947
SARS-CoV-2 Nucleocapsid gene N2	Outcome	nCoV N2 Fwd	TTACAAACATTGGCCGCAAA	29180-29199	67 bp	Lu et al. [4]
		nCoV N2 Rev	GCGCGACATTCCGAAGAA	29246-29228		
		nCoV N2 Probe	FAM-ACAATTTGC-/ZEN/-CCCCAGCGCTTCAG-3IABkFQ	29204-29226		MN908947
Bovine Coronavirus	Process control	BCoV Fwd	CTGGAAGTTGGTGGAGTT	29026-29043	85 bp	Decaro et al. [7]
		BCoV Rev	ATTATCGGCCTAACATACATC	29090-29110		
		BCoV Probe	FAM-CCTTCATATCTATACACATCAAGTTGTT-BHQ-1	29058-29085		U00735
Hepatitis G	Extraction control	HepG Fwd	CGGCCAAAAGGTGGTGGATG	100-119	185 bp	Schlueter et al. [8]
		HepG Rev	CGACGAGCCTGACGTCGGG	285-267		
		HepG Probe	HEX-AGGTCCCTCTGGCGCTTGTGGCGAG-BHQ-1	172-196		U44402
Mouse Beta-actin gene	Reverse-transcription control	Mouse ACTB, 20X VIC	Proprietary, Life Technologies			
Halo-alkaliphilic archaeon gyr *a* gene	Inhibition control	np_gyra Fwd	unpublished			Provided by Josh Steele (SCCWRP)
		np_gyra Rev	unpublished			
		np_gyra Probe	HEX, unpublished			

S1.3. ddPCR Data Interpretation and Quality Control

Amplified droplets were analyzed using a QX200™ instrument (BioRad) according to manufacturer's instructions and data acquisition and analysis were conducted using QuantaSoft™ v. 1.7 (Bio-Rad). Positive and negative droplets were identified by fluorescence amplitude thresholds set manually for each plate [9] and the positive and accepted droplets were pooled across replicate reactions to estimate target concentrations for each sample, excluding individual reactions with fewer than 10,000 accepted droplets or visibly atypical average fluorescence amplitudes. Target copies per µL of ddPCR reaction were converted to copies per L of wastewater by correcting for dilution factors, elution volume, and original volume of sample filtered as follows:

$$X_{ww}[copies/L] = X_{rxn}[copies/\mu L] \times \frac{V_{rxn}\,[\mu L]}{V_{cDNA}\,[\mu L]} \times f_{dilution} \times V_{extract}[\mu L] \times \frac{1}{V_{filtered}[L]}$$

where X_{rxn} is the estimated number of target copies per µL of combined reaction volume V_{rxn} from merged duplicate wells, V_{cDNA} is the volume (in µL) of template cDNA in the combined reactions, $f_{dilution}$ is a unitless RT dilution factor to account for the dilution of extracted RNA when generating cDNA, $V_{extract}$ is the volume (in µL) of RNA eluted from the sample filters through nucleic acid extraction, and $V_{filtered}$ is the volume of wastewater (in L) that was initially filtered.

The limit of detection (LOD) for this procedure was previously determined to be 1070 copies/L wastewater for the N1 assay and 330 copies/L for N2 [1,10]. Briefly, the mean ($\bar{X}$) and standard deviation (σ) of each target quantity were estimated for eight technical replicates of eight wastewater samples (64 reactions total) known *a priori* to be free of SARS-CoV-2. The limit of blank (LOB) was first established as $LOB = \bar{X} + 1.645\sigma$, corresponding to the 95th percentile of the normal distribution [11]; the LOD was then established by adding a further two standard deviations to the LOB (e.g., $LOD = LOB + 2\sigma = \bar{X} + 3.645\sigma$), ensuring that any samples deemed positive provide a signal well in excess of any background fluorescence that could otherwise result in false positives [10,12].Targets

were considered detected and quantifiable in samples with pooled reaction wells containing three or more positive droplets and with target concentrations above the assay-specific LOD.

S2. Exponential Kernel Smoothing Function

We defined the following **R** function to implement univariate exponential kernel smoothing for this analysis utilizing the rdist() function from the *fields* package [13,14]. For n observations with locations given by the n-length vector x and values in a second vector y, the function returns an n-length vector $\hat{y}$ containing the smoothed estimates for each observation. Detrended residuals can be computed by subtracting each element of $\hat{y}$ from the corresponding value in y.

Code Block S1. Exponential Kernel Smoothing **R** Function

```
ks_exp_loop <- function(x, y, range){
  # x is the observed location (e.g. date)
  # y is the observed value (e.g. cases)

  n <- length(x)
  y_hat <- rep(NA, n)  # set up object to hold smooth estimates

  for(i in 1:n){
    x_dist <- fields::rdist(x[i], x)
    x_wt <- exp(-3*x_dist/range)  # weights from exponential decay function
    x_sum <- rowSums(x_wt,na.rm = TRUE)  # sum the weights for each location
    x_norm <- x_wt / x_sum  # normalize the weights for each location by their sum

    y_hat[i] <- sum(x_norm * y, na.rm = TRUE)  # smoothed estimate
  }

  return(y_hat)
}
```

S3. Sewershed Wastewater Viral Loads and COVID-19 Incidence

The range of COVID-19 incidence rates and SARS-CoV-2 wastewater viral loads observed in each sewershed are presented in Table S2. COVID-19 incidence and wastewater viral loads reported on the same day were significantly correlated ($p < 0.001$) for all sewersheds except the two smallest by population, Newport and Pittsboro.

Table S2. Summary statistics by sewershed of COVID-19 incidence rates, wastewater SARS-CoV-2 loads, and their correlation

Sewershed	COVID-19 Incidence (cases/100,000 population)			Wastewater Viral Load (log_{10} GC/person/day)			Spearman's Correlation	
	Median	SD[a]	Range[b]	Median	SD	Range	ρ	p-value
Beaufort	42.1	43.3	0.0, 228.6	14.0	1.9	11.9, 17.8	0.38	<0.001
Charlotte 1	21.8	24.8	0.0, 132.5	15.6	1.5	11.3, 17.7	0.85	<0.001
Charlotte 2	17.5	18.6	0.0, 105.2	15.7	1.4	11.6, 17.7	0.81	<0.001
Charlotte 3	26.3	22.7	0.0, 84.2	16.6	1.1	13.6, 18.1	0.74	<0.001
Wilson	20.2	27.3	4.0, 125.5	15.6	1.7	12.2, 17.9	0.78	<0.001
Fayetteville	30.0	22.3	3.3, 99.6	16.1	1.6	11.8, 19.9	0.72	<0.001
Greensboro	19.9	18.2	0.0, 69.2	15.7	1.9	11.5, 17.7	0.67	<0.001
Greenville	23.4	30.7	0.0, 196.4	15.6	1.4	11.8, 18.3	0.80	<0.001
Laurinburg	12.9	30.4	0.0, 128.8	15.9	1.5	12.0, 18.0	0.71	<0.001
Marion	23.6	50.9	0.0, 212.8	15.9	2.0	11.2, 18.2	0.58	<0.001
MSD of Buncombe County	26.0	22.0	0.0, 82.7	15.6	1.5	11.5, 16.9	0.82	<0.001
Newport	0.0	27.7	0.0, 188.5	11.8	1.1	11.3, 15.4	0.21	0.09
Chapel Hill	7.7	13.1	0.0, 67.8	14.6	1.8	11.4, 17.4	0.84	<0.001
Pittsboro	0.0	27.8	0.0, 141.7	12.6	1.5	11.7, 16.6	0.34	0.03
Raleigh	19.7	23.5	0.0, 136.9	14.8	1.6	11.4, 17.8	0.84	<0.001
Roanoke Rapids	34.9	43.3	0.0, 195.5	16.1	1.8	12.2, 18.8	0.64	<0.001
South Durham	12.0	13.7	0.0, 74.0	14.5	1.7	11.0, 17.0	0.69	<0.001
Wilmington	24.0	33.0	0.0, 231.3	14.5	1.8	10.8, 18.0	0.71	<0.001
New Hanover County	14.8	18.3	0.0, 82.7	14.0	2.0	10.7, 17.9	0.50	<0.001
Winston-Salem	23.6	24.4	1.1, 88.8	15.4	1.9	11.1, 17.4	0.82	<0.001

[a] standard deviation
[b] minimum, maximum

S4. Site-Specific Cross-Correlations

Spearman's correlation estimates between wastewater concentrations and COVID-19 incidence rates at each temporal lag (τ = -7 days to +7 days) after detrending with each smoothing range considered (T = ∞, 16, 8, 4, and 2 weeks) are presented separately for each WWTP (Figure S2 - Figure S21). A summary of the identified optimal smoothing range, relationship, span, and temporal offset with the highest correlation is also presented for each sewershed (Table S3).

Table S3. Summary of the optimal smoothing range, timing relationship of wastewater to cases, span of temporal offsets significant for the timing relationship between wastewater and cases, and the temporal offset with the highest correlation identified according to the proposed criteria for each sewershed

Sewershed	Optimal Smoothing Range	Timing of Wastewater Relative to Cases	Span of Significant Temporal Offsets (days)	Temporal Offset with Highest Correlation (days)
Beaufort	∞ weeks	Lead	-7:-4	-6
Charlotte 1	8 weeks	Lead	-3:0	0
Charlotte 2	4 weeks	Lag	3:4	4
Charlotte 3	4 weeks	Lead	-6:-4	-6
Wilson	Inconclusive	Inconclusive	N/A	N/A
Fayetteville	4 weeks	Lag	2:3	3
Greensboro	8 weeks	Lead	-7:-6	-7
Greenville	8 weeks	Lead	-7:-3	-7
Laurinburg	Inconclusive	Inconclusive	N/A	N/A
Marion	Inconclusive	Inconclusive	N/A	N/A
MSD of Buncombe County	Inconclusive	Inconclusive	N/A	N/A
Newport	4 weeks	Lag	6:7	6
Chapel Hill	8 weeks	Lag	0:2	0
Pittsboro	∞ weeks	Lead	-1:0	-1
Raleigh	8 weeks	Lead	-2:1	0
Roanoke Rapids	Inconclusive	Inconclusive	N/A	N/A
South Durham	8 weeks	Lead	-7:-6	-6
Wilmington	8 weeks	Lead	-7:-4	-7
New Hanover County	16 weeks	Lead	-7:-5	-6
Winston-Salem	8 weeks	Lead	-1:0	0

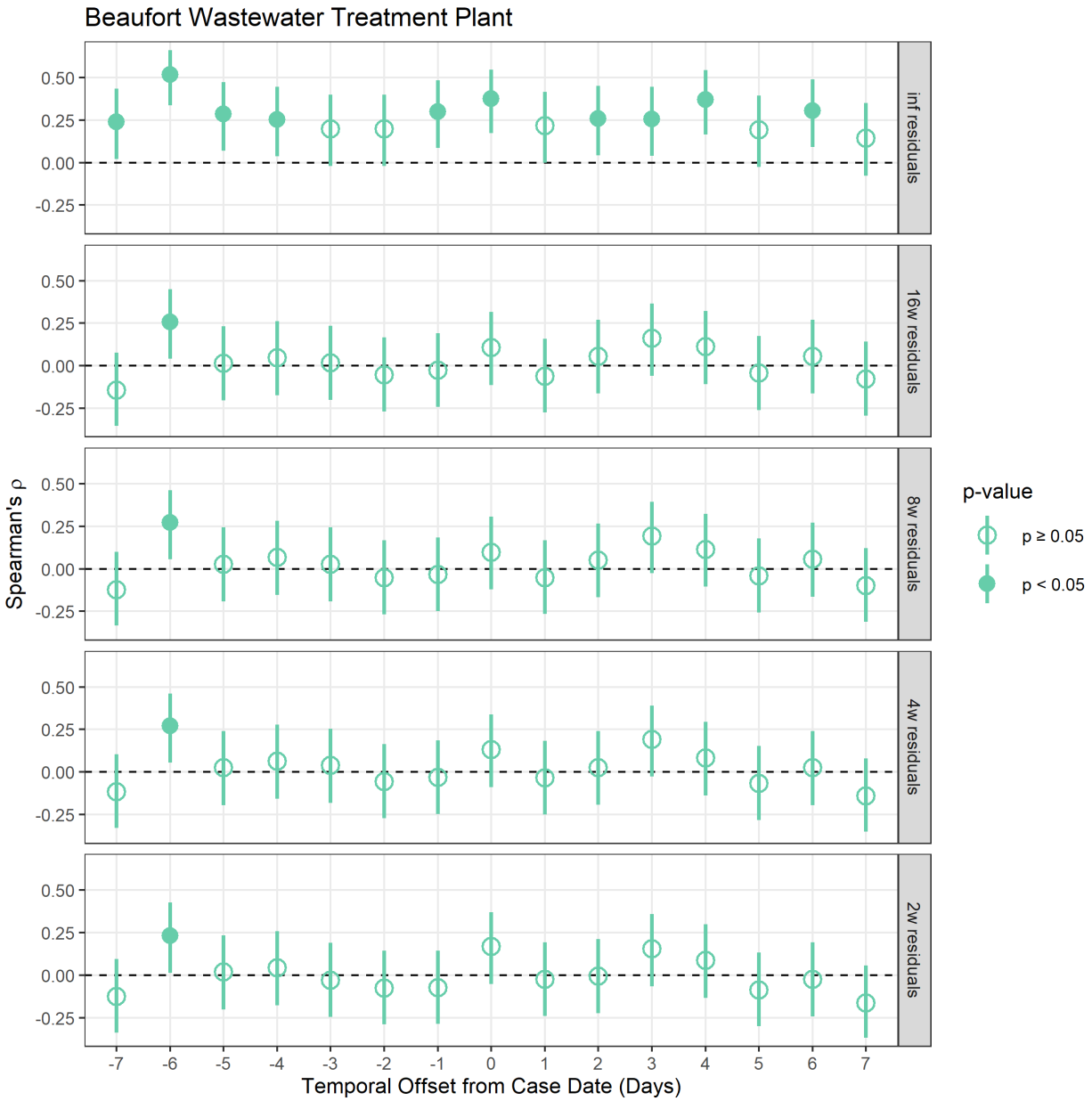

Figure S2. Beaufort sewershed COVID-19 incidence rate cross-correlation plots with wastewater viral load for smoothing ranges of ∞, 16, 8, 4, and 2 weeks

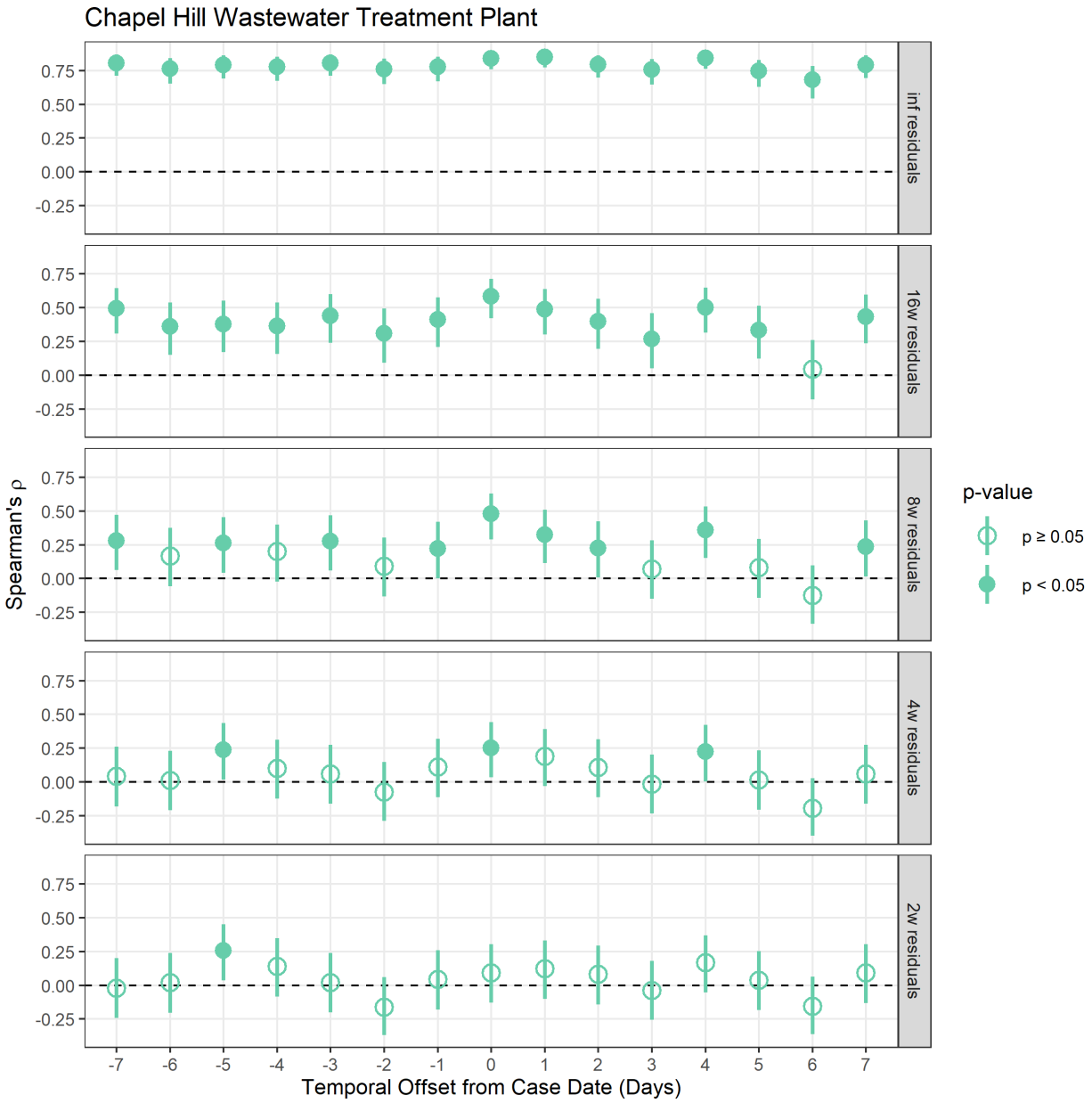

Figure S3. Chapel Hill sewershed COVID-19 incidence rate cross-correlation plots with wastewater viral load for smoothing ranges of ∞, 16, 8, 4, and 2 weeks

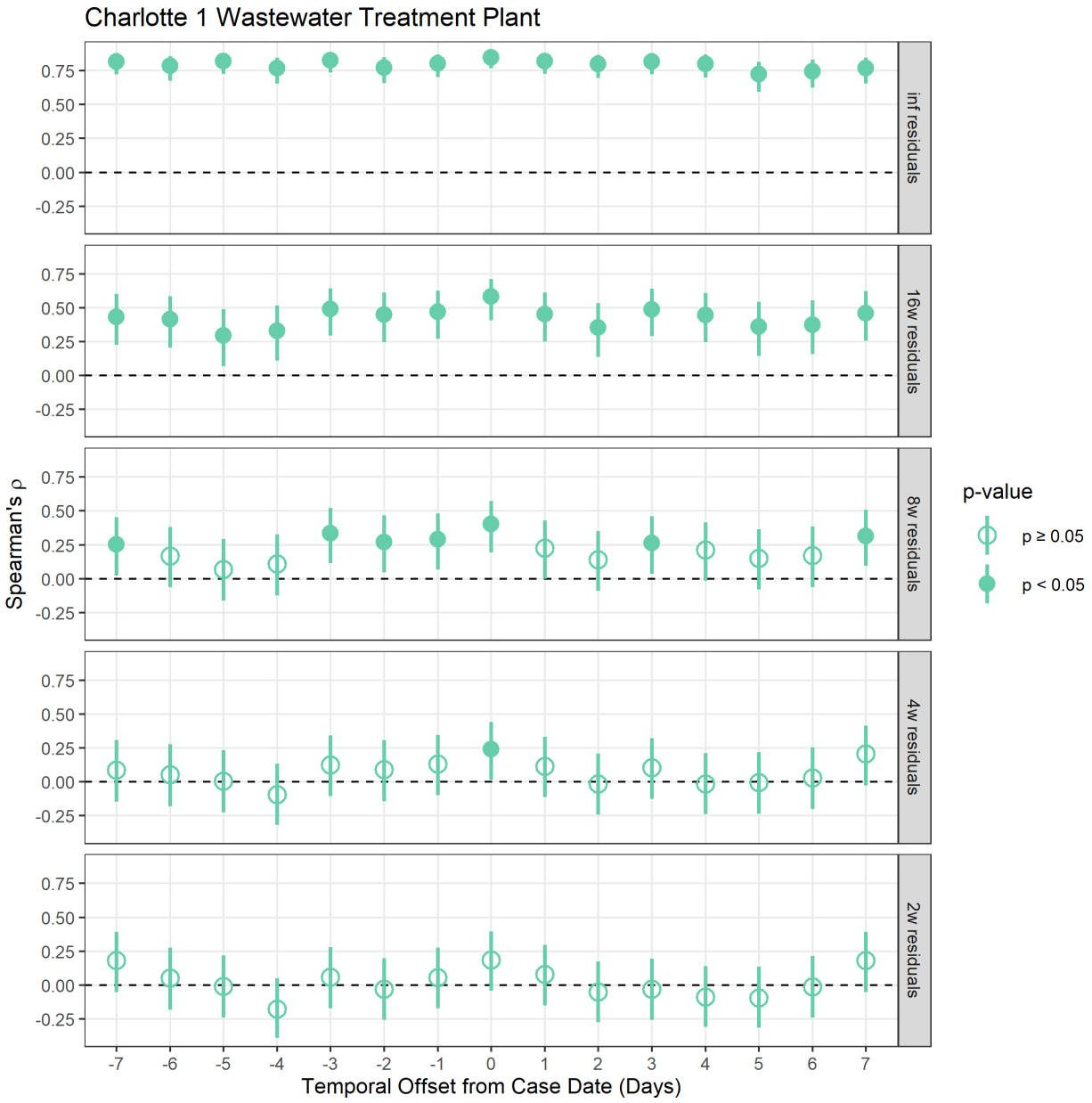

Figure S4. Charlotte 1 sewershed COVID-19 incidence rate cross-correlation plots with wastewater viral load for smoothing ranges of ∞, 16, 8, 4, and 2 weeks

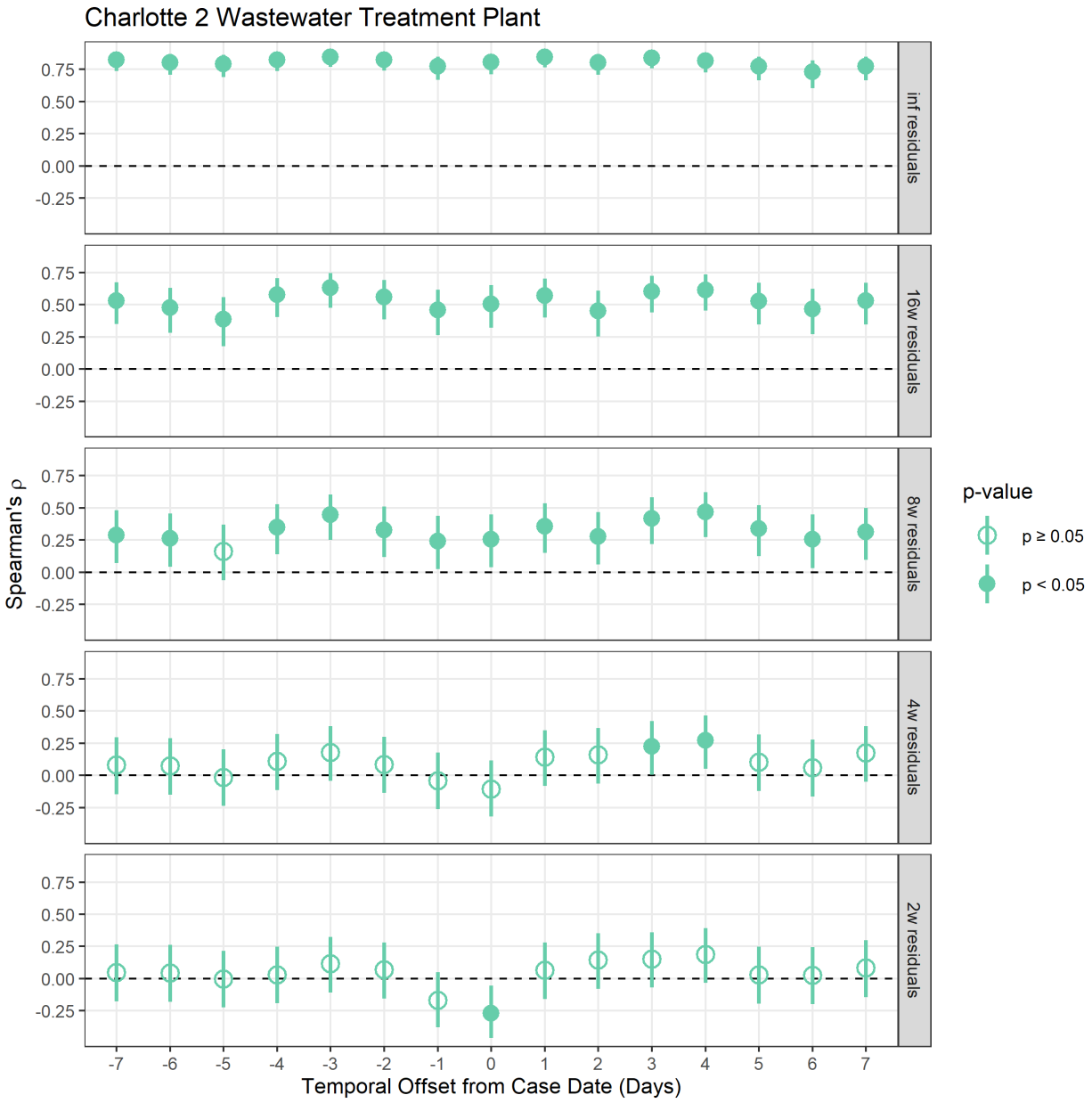

Figure S5. Charlotte 2 sewershed COVID-19 incidence rate cross-correlation plots with wastewater viral load for smoothing ranges of ∞, 16, 8, 4, and 2 weeks

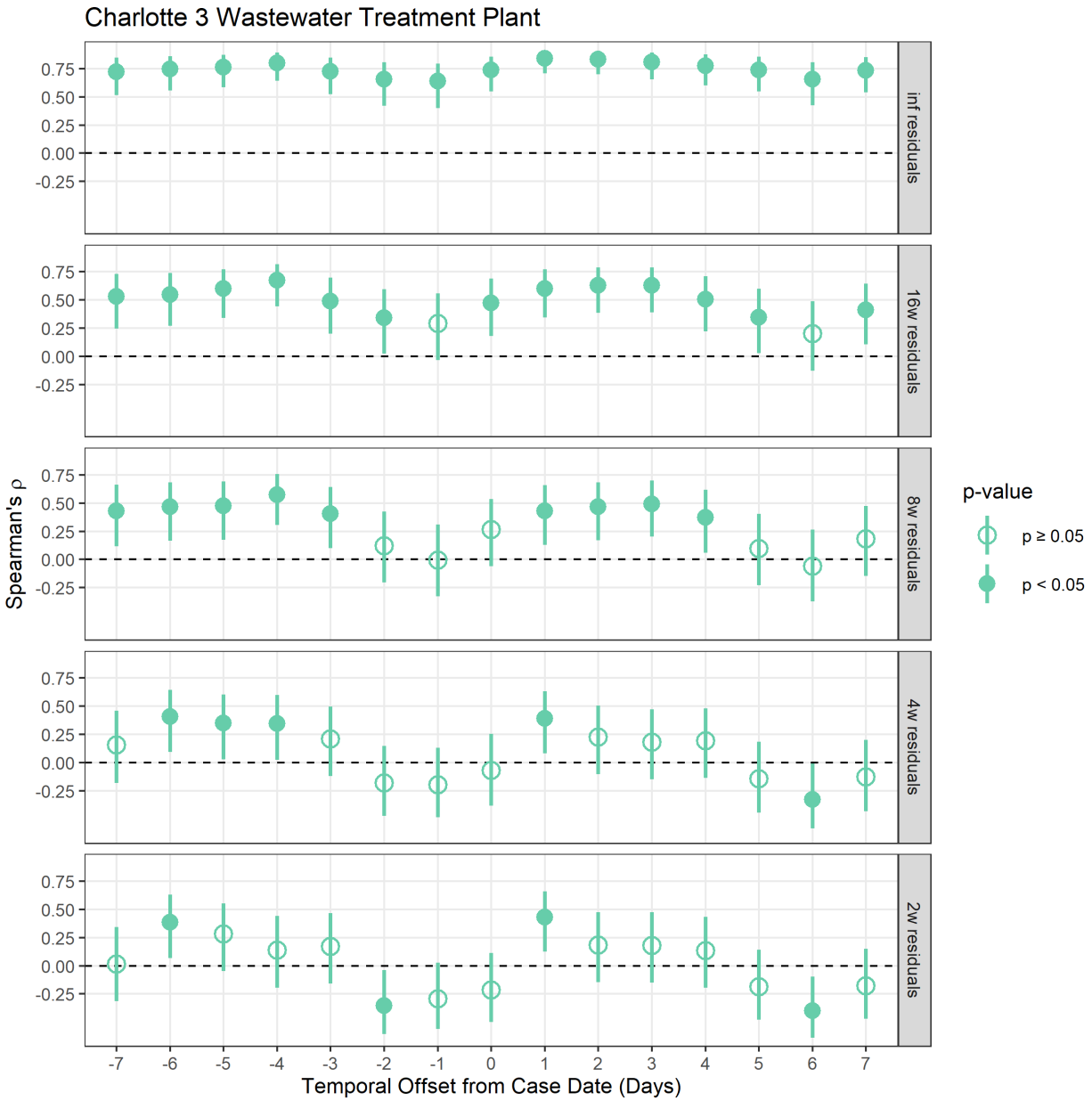

Figure S6. Charlotte 3 sewershed COVID-19 incidence rate cross-correlation plots with wastewater viral load for smoothing ranges of ∞, 16, 8, 4, and 2 weeks

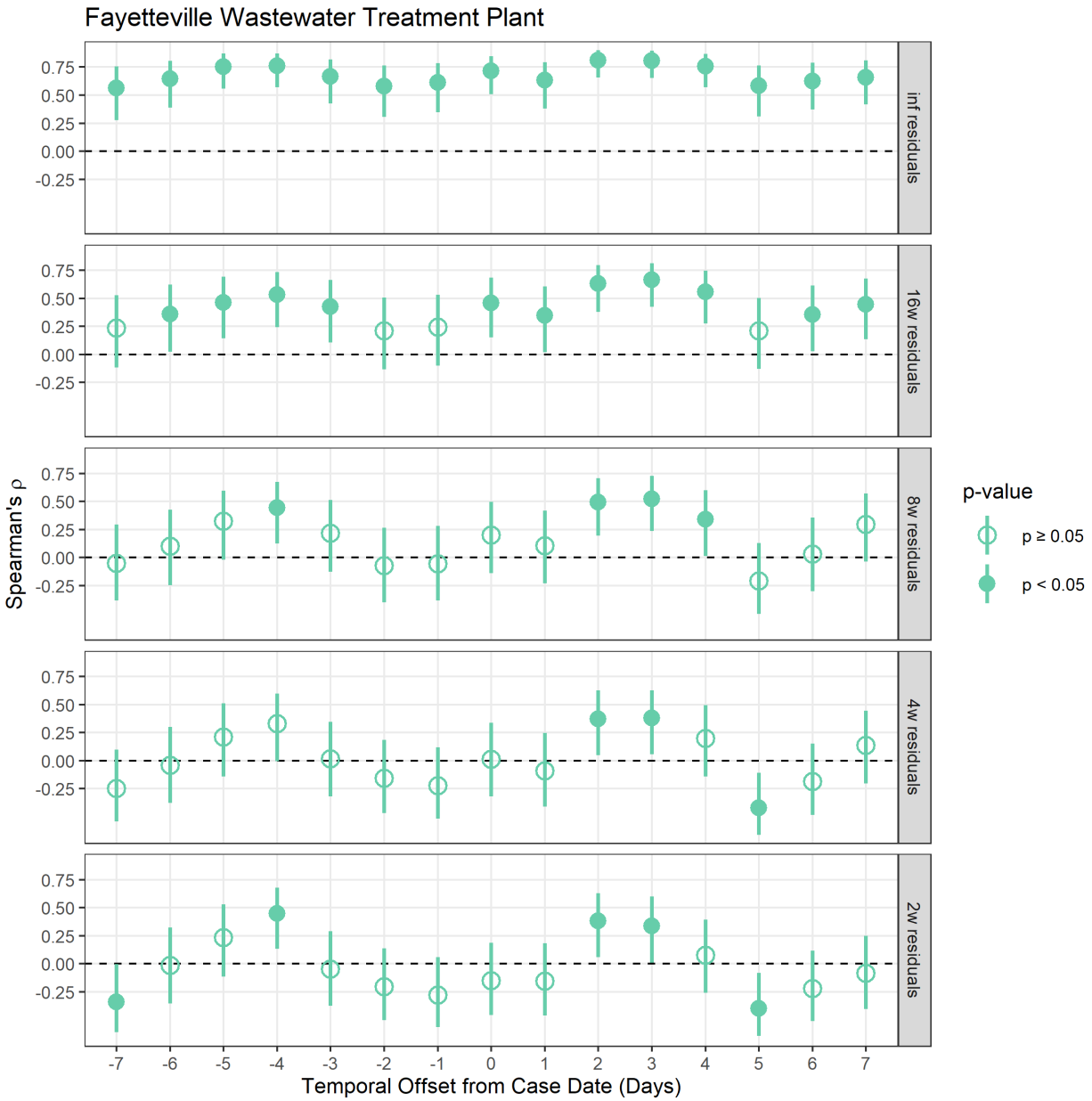

Figure S7. Fayetteville sewershed COVID-19 incidence rate cross-correlation plots with wastewater viral load for smoothing ranges of ∞, 16, 8, 4, and 2 weeks

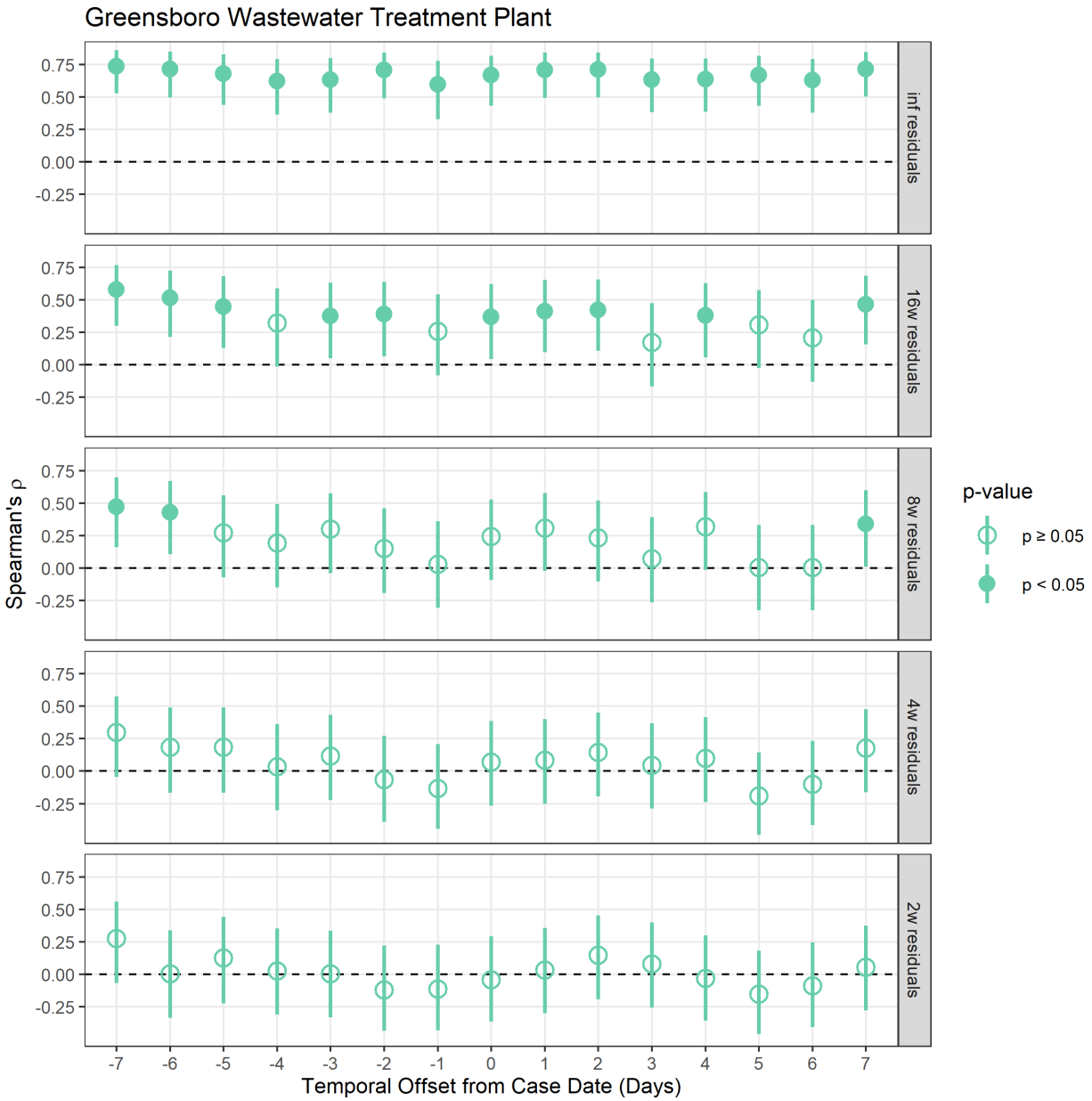

Figure S8. Greensboro sewershed COVID-19 incidence rate cross-correlation plots with wastewater viral load for smoothing ranges of ∞, 16, 8, 4, and 2 weeks

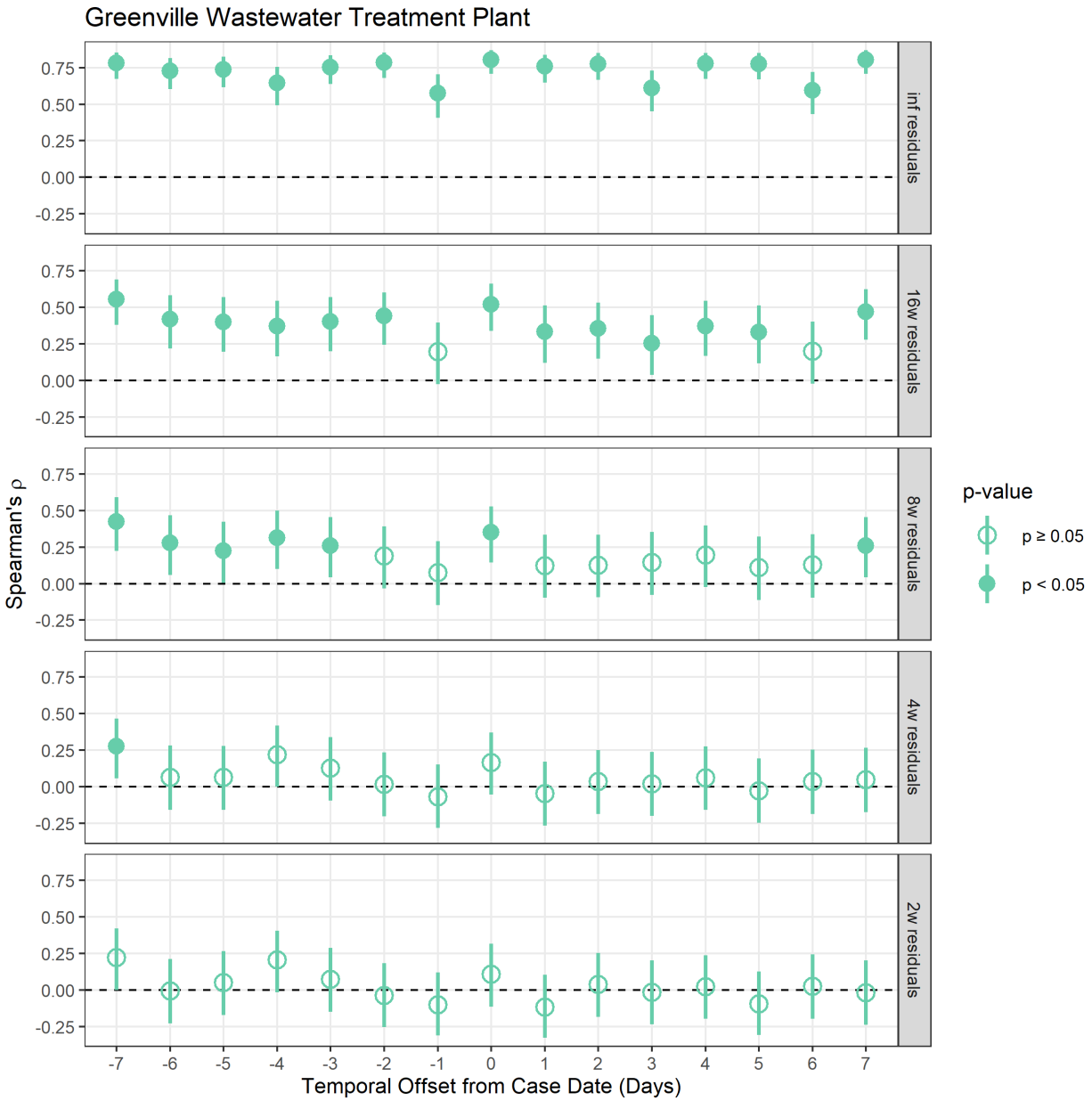

Figure S9. Greenville sewershed COVID-19 incidence rate cross-correlation plots with wastewater viral load for smoothing ranges of ∞, 16, 8, 4, and 2 weeks

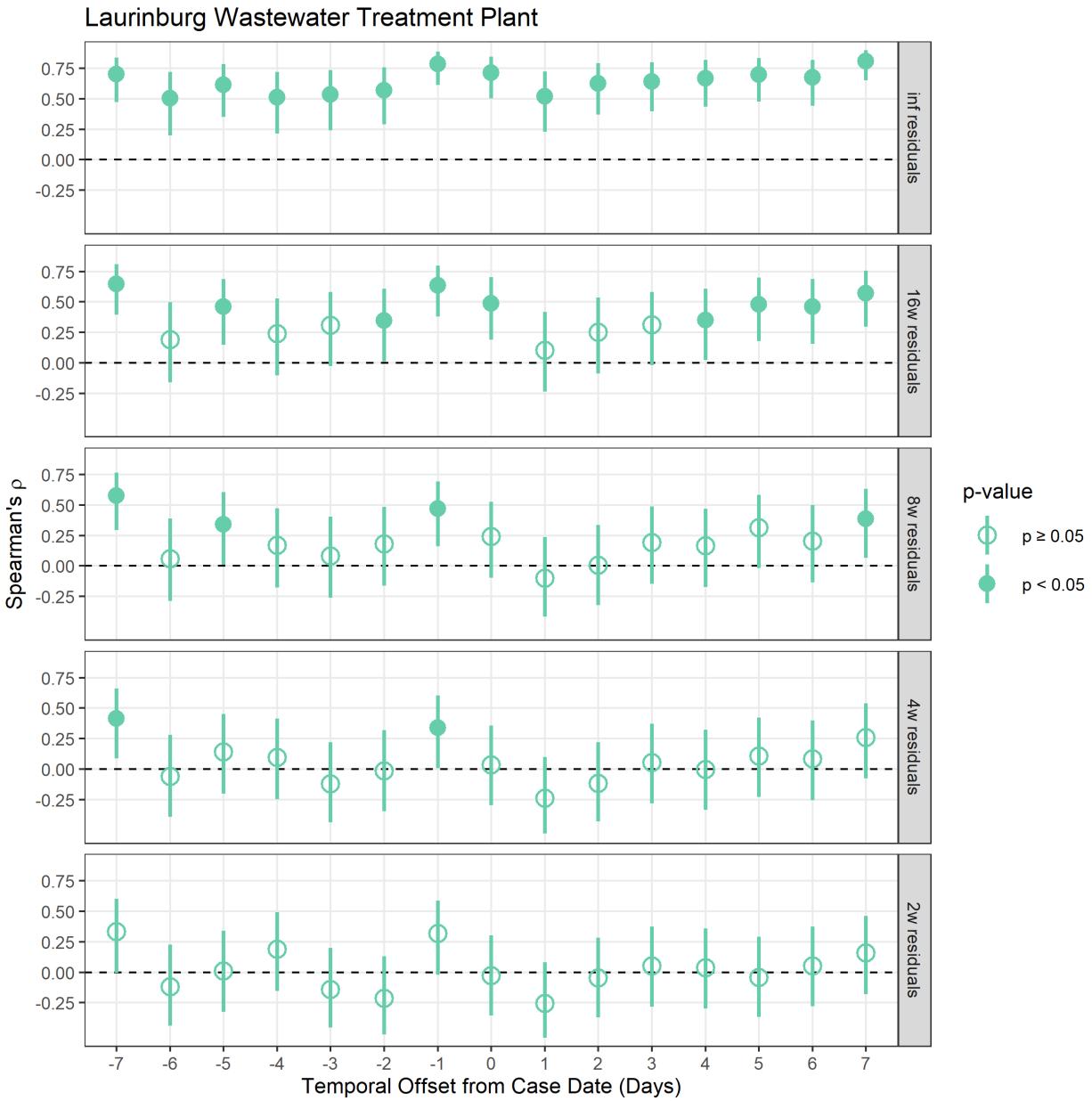

Figure S10. Laurinburg sewershed COVID-19 incidence rate cross-correlation plots with wastewater viral load for smoothing ranges of ∞, 16, 8, 4, and 2 weeks

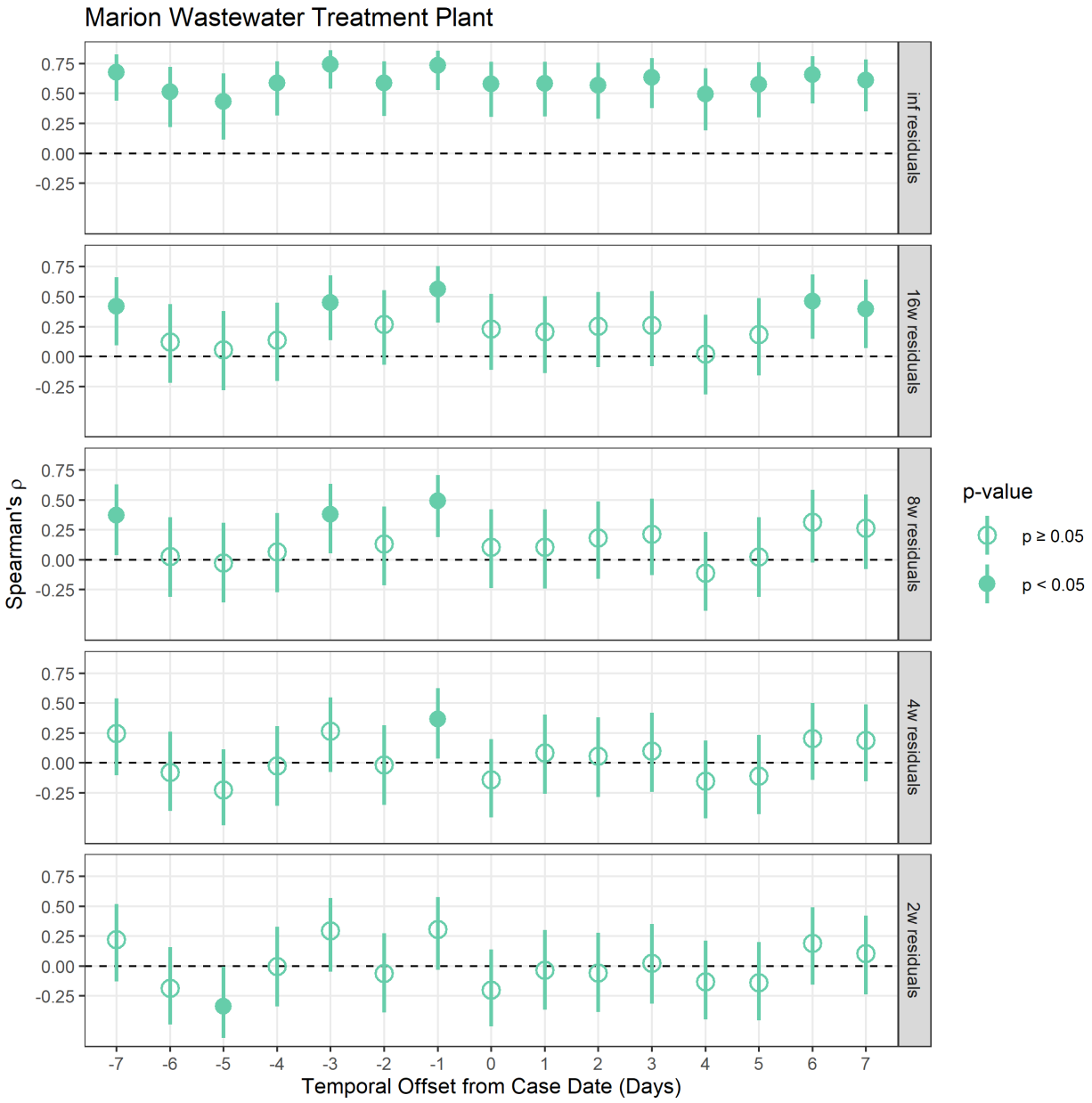

Figure S11. Marion sewershed COVID-19 incidence rate cross-correlation plots with wastewater viral load for smoothing ranges of ∞, 16, 8, 4, and 2 weeks

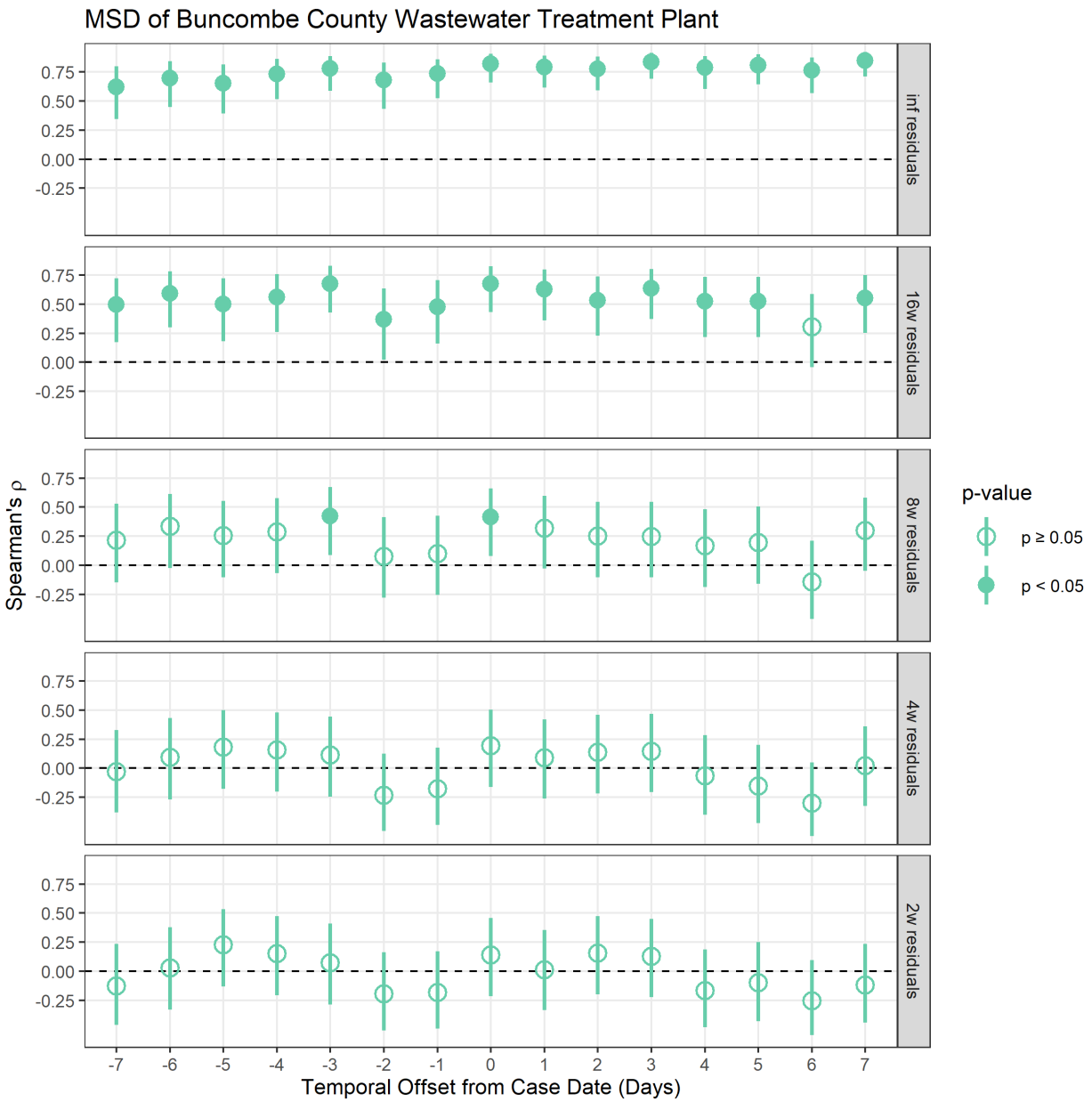

Figure S12. MSD of Buncombe County sewershed COVID-19 incidence rate cross-correlation plots with wastewater viral load for smoothing ranges of ∞, 16, 8, 4, and 2 weeks

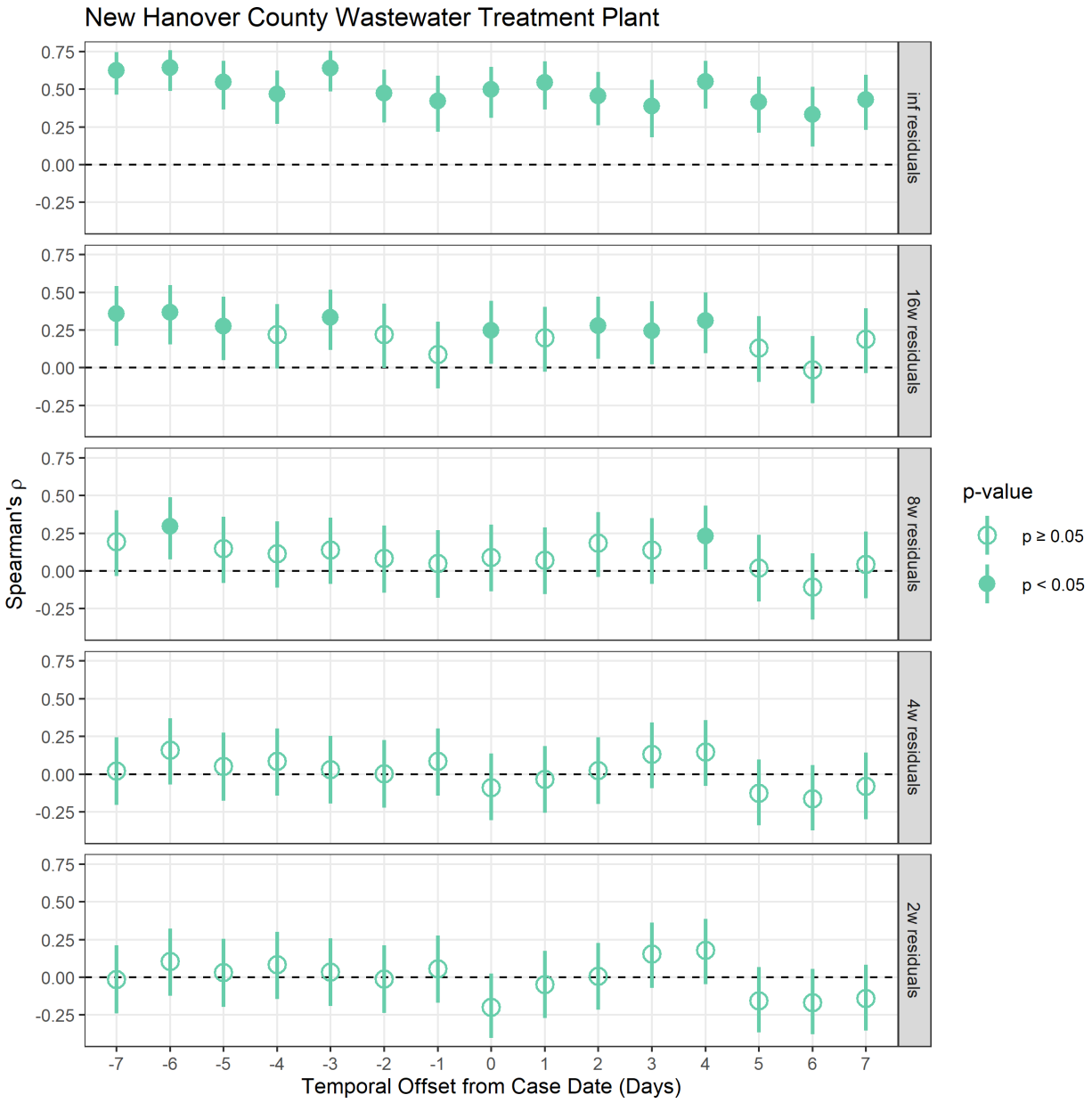

Figure S13. New Hanover County sewershed COVID-19 incidence rate cross-correlation plots with wastewater viral load for smoothing ranges of ∞, 16, 8, 4, and 2 weeks

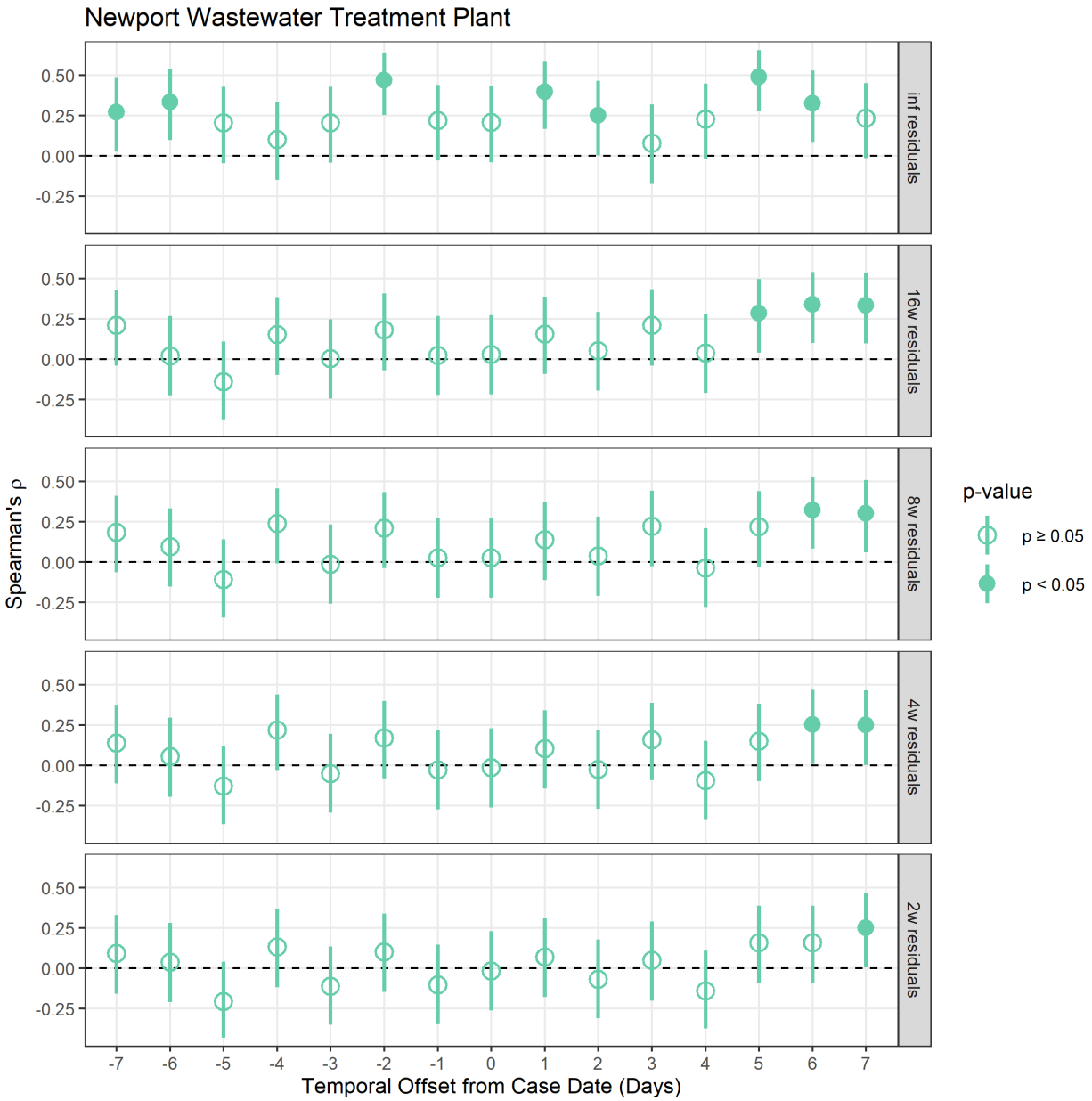

Figure S14. Newport sewershed COVID-19 incidence rate cross-correlation plots with wastewater viral load for smoothing ranges of ∞, 16, 8, 4, and 2 weeks

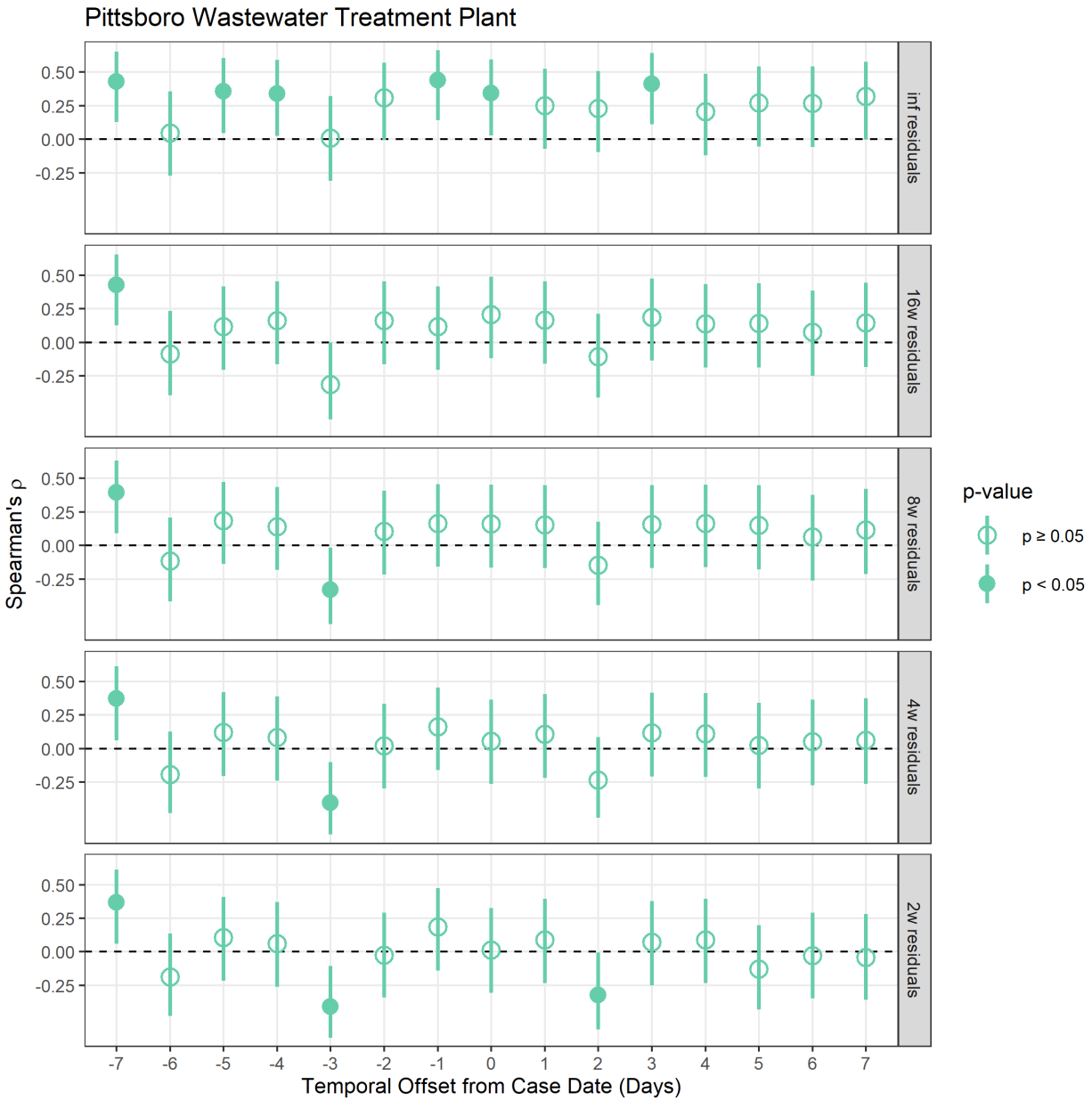

Figure S15. Pittsboro sewershed COVID-19 incidence rate cross-correlation plots with wastewater viral load for smoothing ranges of ∞, 16, 8, 4, and 2 weeks

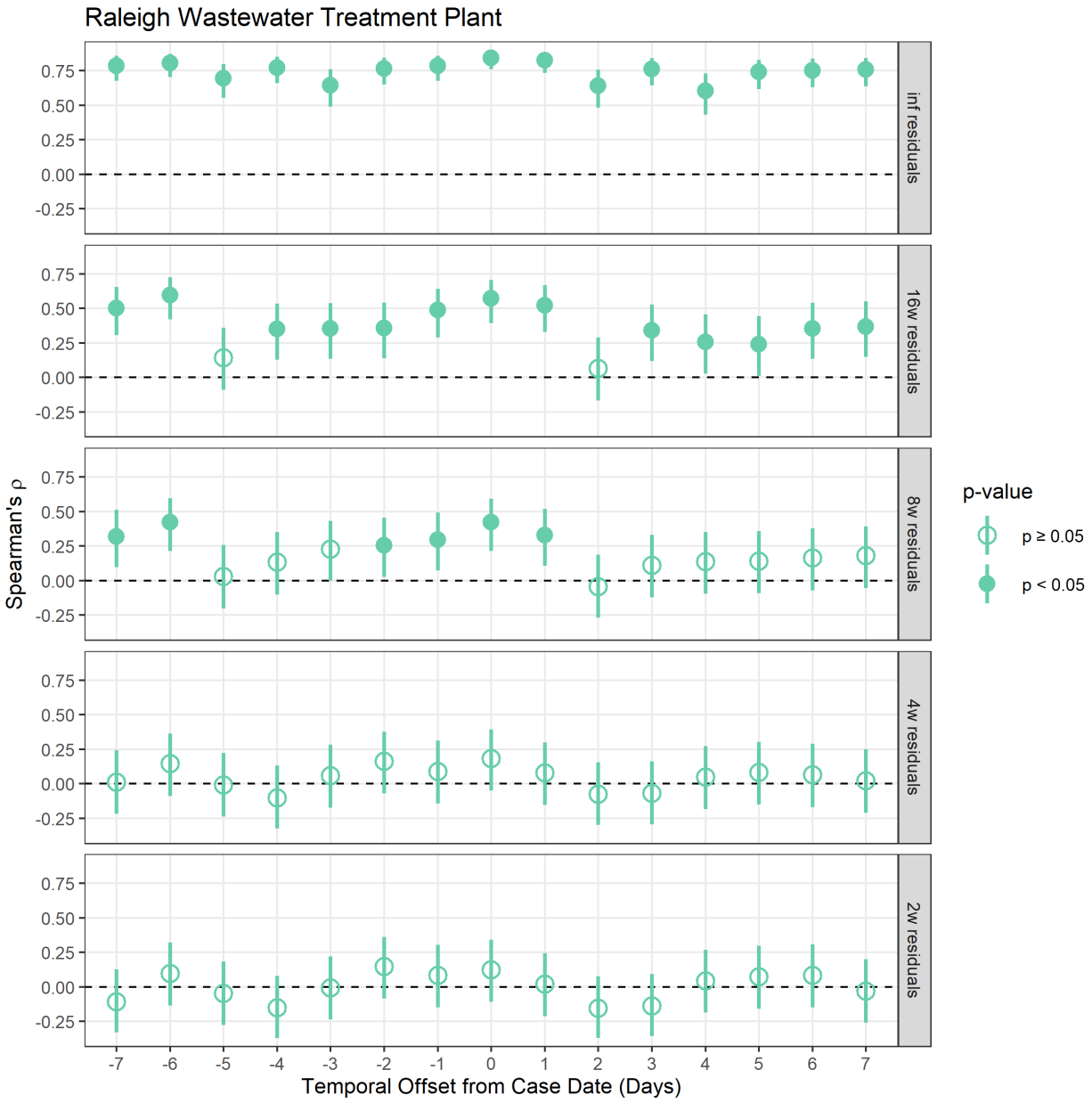

Figure S16. Raleigh sewershed COVID-19 incidence rate cross-correlation plots with wastewater viral load for smoothing ranges of ∞, 16, 8, 4, and 2 weeks

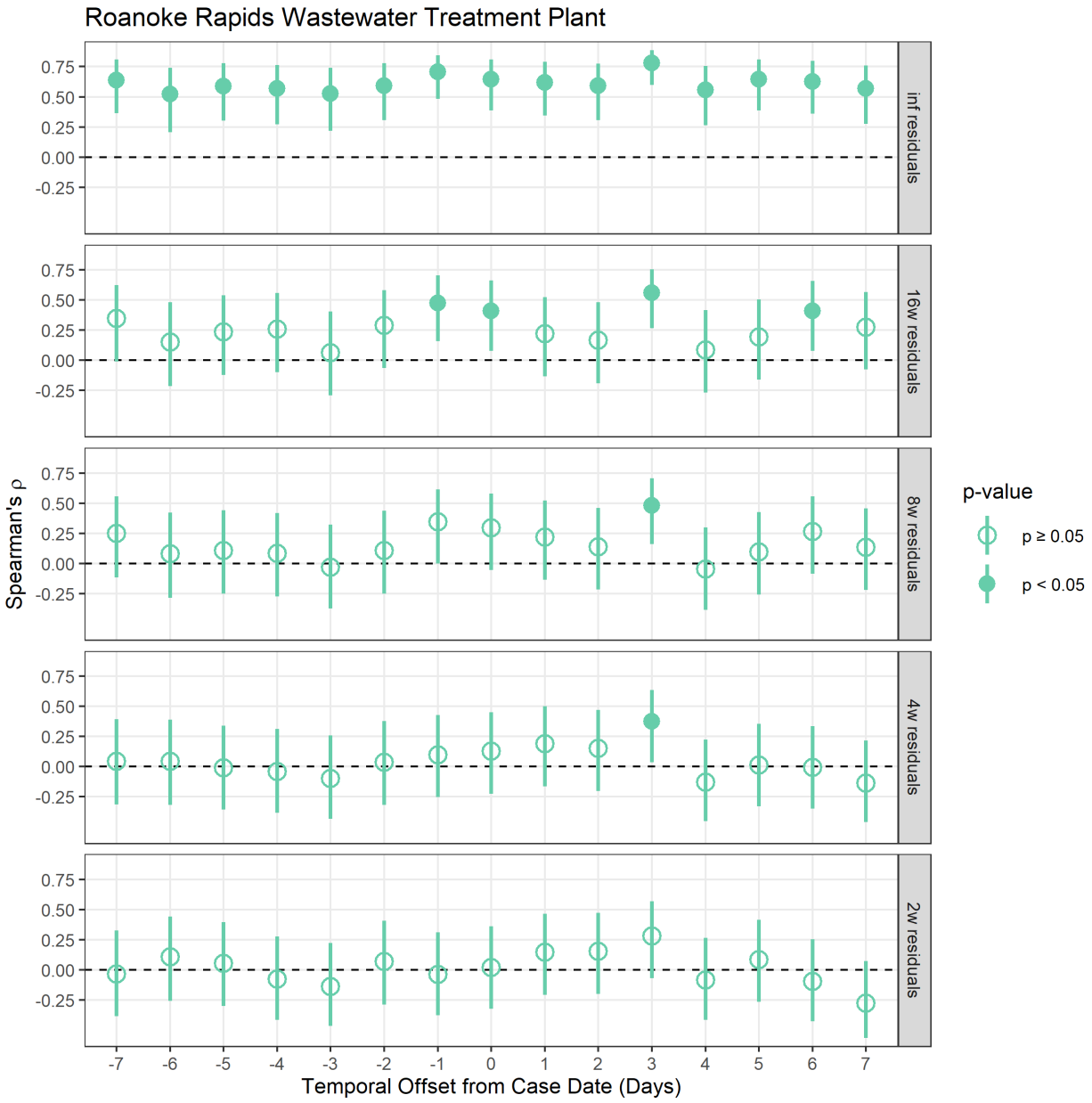

Figure S17. Roanoke Rapids sewershed COVID-19 incidence rate cross-correlation plots with wastewater viral load for smoothing ranges of ∞, 16, 8, 4, and 2 weeks

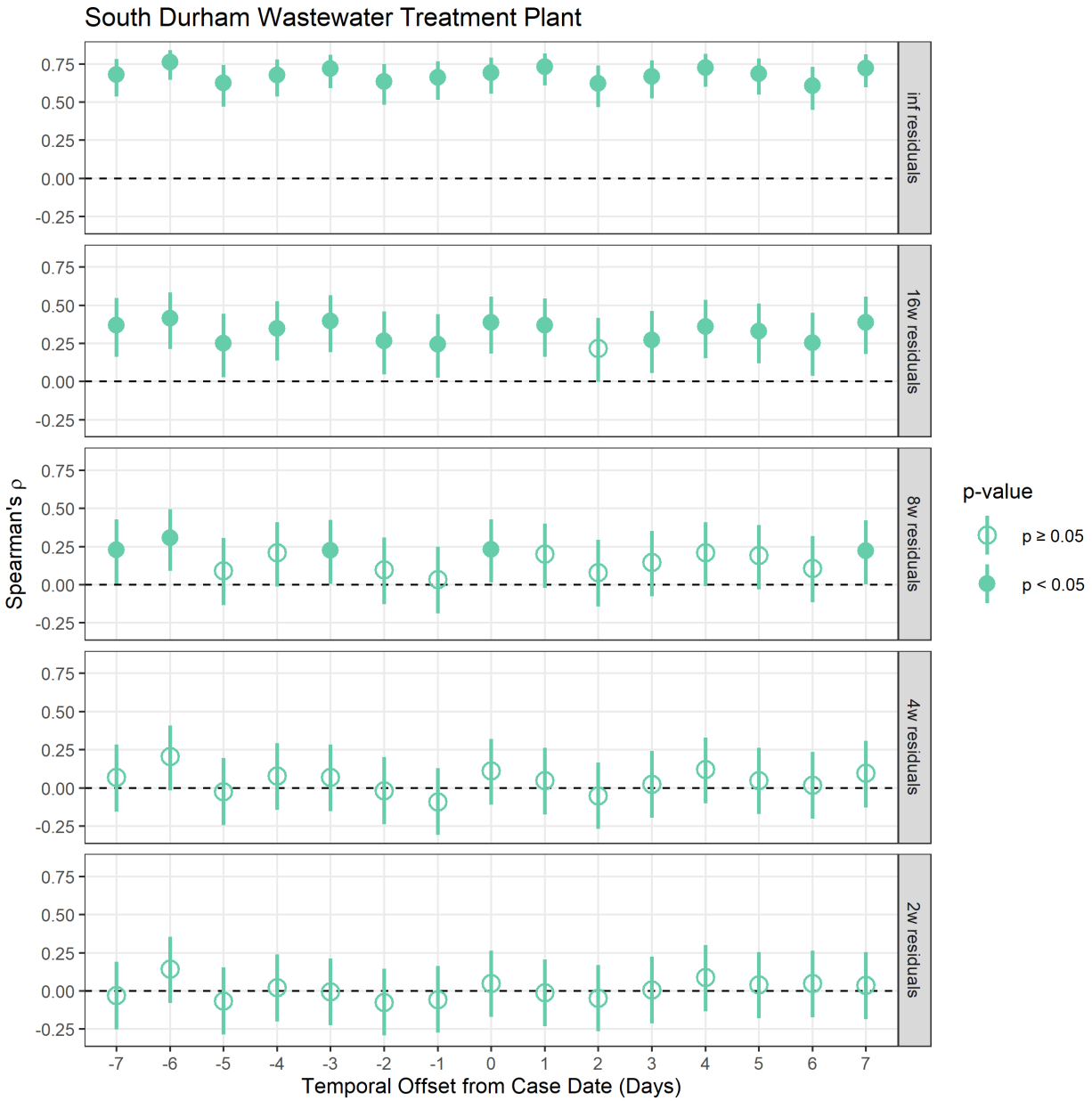

Figure S18. South Durham sewershed COVID-19 incidence rate cross-correlation plots with wastewater viral load for smoothing ranges of ∞, 16, 8, 4, and 2 weeks

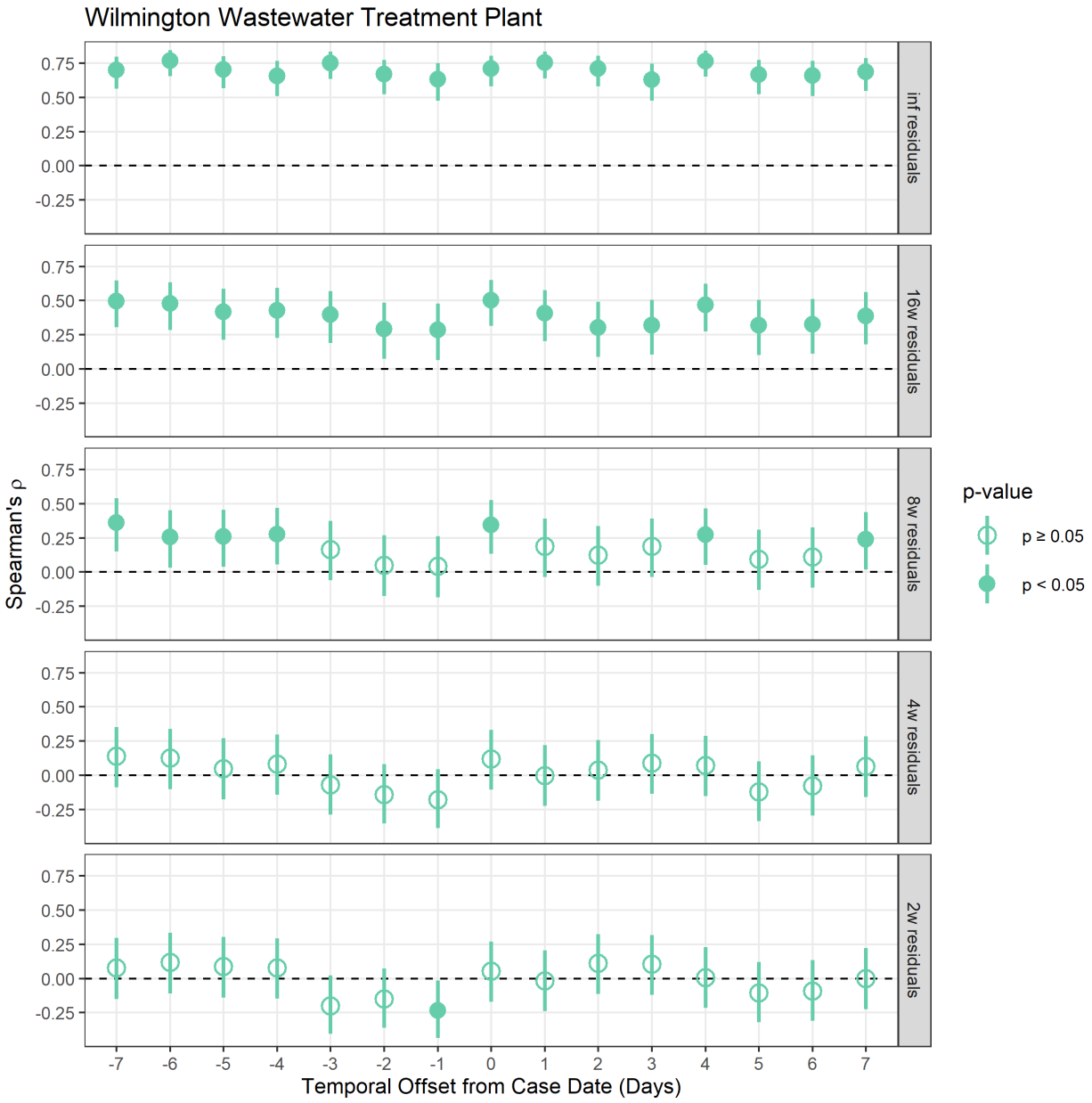

Figure S19. Wilmington sewershed COVID-19 incidence rate cross-correlation plots with wastewater viral load for smoothing ranges of ∞, 16, 8, 4, and 2 weeks

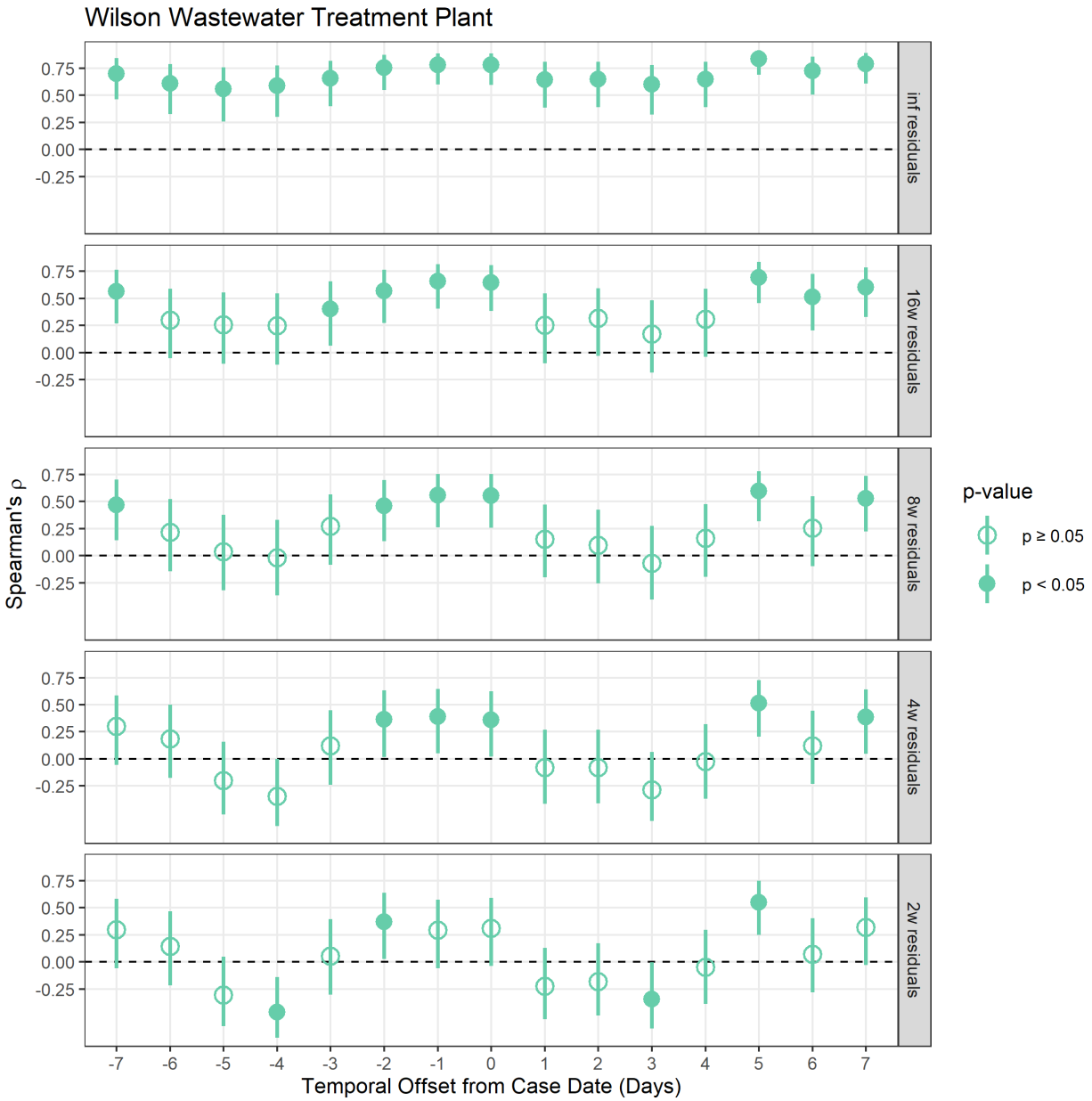

Figure S20. Wilson sewershed COVID-19 incidence rate cross-correlation plots with wastewater viral load for smoothing ranges of ∞, 16, 8, 4, and 2 weeks

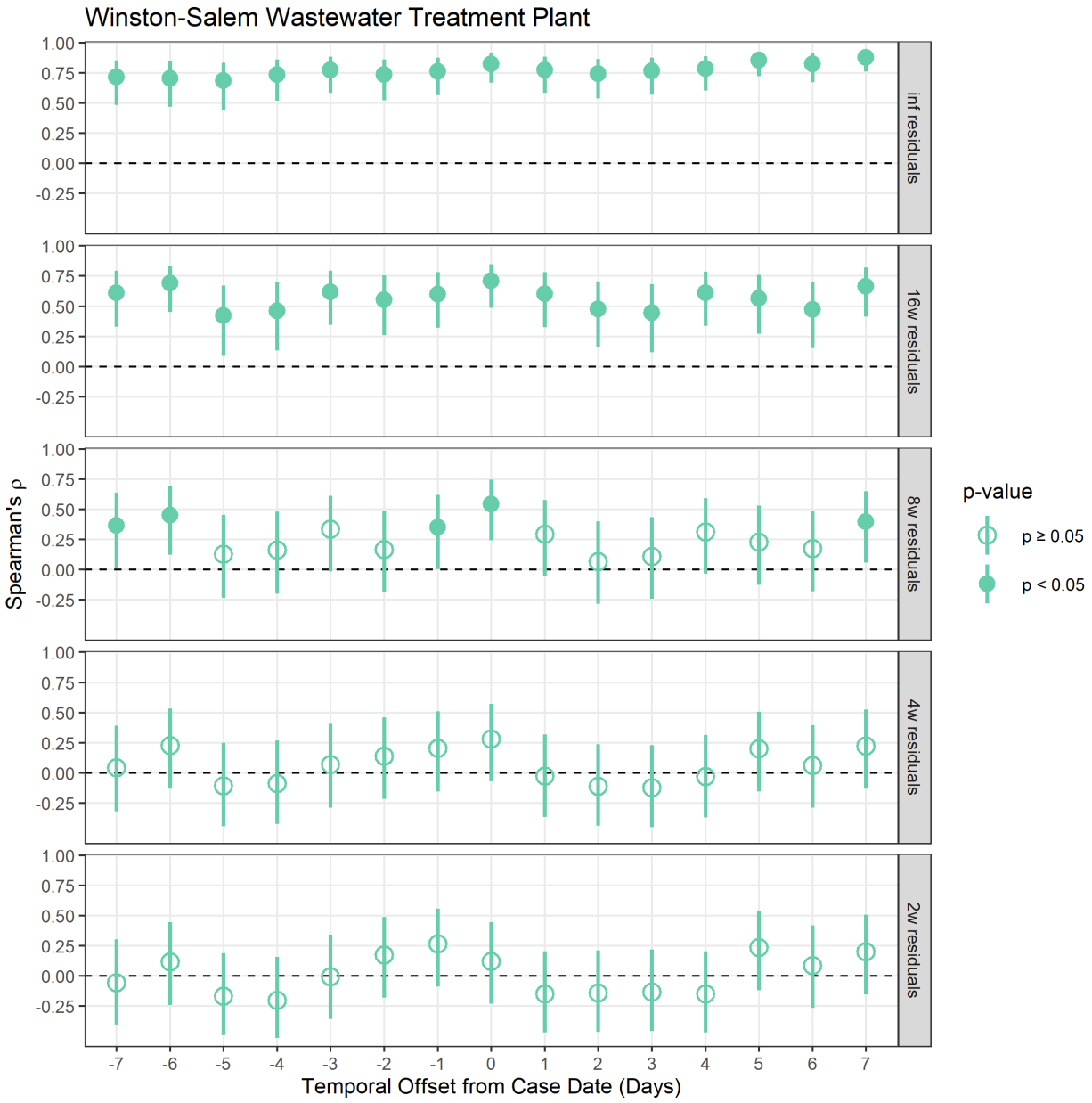

Figure S21. Winston-Salem sewershed COVID-19 incidence rate cross-correlation plots with wastewater viral load for smoothing ranges of ∞, 16, 8, 4, and 2 weeks

S5. Supplementary References

1. Beattie RE, Blackwood AD, Clerkin T, Dinga C, Noble RT. Evaluating the impact of sample storage, handling, and technical ability on the decay and recovery of SARS-CoV-2 in wastewater. PLOS ONE. 2022;17: 1–16. doi:10.1371/journal.pone.0270659

2. CDC. Wastewater Surveillance Testing Methods. In: Centers for Disease Control and Prevention [Internet]. 26 Jan 2022 [cited 27 Jul 2022]. Available: https://www.cdc.gov/healthywater/surveillance/wastewater-surveillance/testing-methods.html

3. Katayama H, Shimasaki A, Ohgaki S. Development of a Virus Concentration Method and Its Application to Detection of Enterovirus and Norwalk Virus from Coastal Seawater. Applied and Environmental Microbiology. 2002;68: 1033–1039. doi:10.1128/AEM.68.3.1033-1039.2002

4. Lu X, Wang L, Sakthivel SK, Whitaker B, Murray J, Kamili S, et al. US CDC Real-Time Reverse Transcription PCR Panel for Detection of Severe Acute Respiratory Syndrome Coronavirus 2. Emerging Infectious Diseases. 2020;26: 1654–1665. doi:10.3201/eid2608.201246

5. Borchardt MA, Boehm AB, Salit M, Spencer SK, Wigginton KR, Noble RT. The Environmental Microbiology Minimum Information (EMMI) Guidelines: qPCR and dPCR Quality and Reporting for Environmental Microbiology. Environmental Science & Technology. 2021. doi:10.1021/acs.est.1c01767

6. dMIQE Group, Huggett JF. The Digital MIQE Guidelines Update: Minimum Information for Publication of Quantitative Digital PCR Experiments for 2020. Clinical Chemistry. 2020;66: 1012–1029. doi:10.1093/clinchem/hvaa125

7. Decaro N, Elia G, Campolo M, Desario C, Mari V, Radogna A, et al. Detection of bovine coronavirus using a TaqMan-based real-time RT-PCR assay. Journal of Virological Methods. 2008;151: 167–171. doi:10.1016/j.jviromet.2008.05.016

8. Schlueter V, Schmolke S, Stark K, Hess G, Ofenloch-Haehnle B, Engel AM. Reverse transcription-PCR detection of hepatitis G virus. Journal of Clinical Microbiology. 1996;34: 2660–2664. doi:10.1128/jcm.34.11.2660-2664.1996

9. Dobnik D, Štebih D, Blejec A, Morisset D, Žel J. Multiplex quantification of four DNA targets in one reaction with Bio-Rad droplet digital PCR system for GMO detection. Scientific Reports. 2016;6: 35451. doi:10.1038/srep35451

10. Ciesielski M, Blackwood D, Clerkin T, Gonzalez R, Thompson H, Larson A, et al. Assessing sensitivity and reproducibility of RT-ddPCR and RT-qPCR for the quantification of SARS-CoV-2 in wastewater. Journal of Virological Methods. 2021;297: 114230. doi:10.1016/j.jviromet.2021.114230

11. Armbruster DA, Pry T. Limit of blank, limit of detection and limit of quantitation. The Clinical Biochemist Reviews. 2008;29 Suppl 1: S49-52.

12. Hayden RT, Gu Z, Ingersoll J, Abdul-Ali D, Shi L, Pounds S, et al. Comparison of Droplet Digital PCR to Real-Time PCR for Quantitative Detection of Cytomegalovirus. Journal of Clinical Microbiology. 2013;51: 540–546. doi:10.1128/JCM.02620-12

13. Nychka D, Furrer R, Paige J, Sain S. fields: Tools for spatial data. Boulder, CO, USA; 2021. Available: https://github.com/dnychka/fieldsRPackage

14. R Core Team. R: A Language and Environment for Statistical Computing. Vienna, Austria: R Foundation for Statistical Computing; 2021. Available: https://www.R-project.org/